Journal of Building Engineering 97 (2024) 110737

Contents lists available at ScienceDirect

Journal of Building Engineering

journal homepage: www.elsevier.com/locate/jobe

Drying shrinkage and crack width prediction using machine learning in mortars containing different types of industrial by-product fine aggregates

Ayla Ocak [a], Gebrail Bekdaş [a,*], Ümit Işıkdağ [b], Sinan Melih Nigdeli [a], Turhan Bilir [a]

[a] Department of Civil Engineering, Istanbul University - Cerrahpaşa, Istanbul, 34320, Turkey
[b] Department of Architecture, Mimar Sinan Fine Arts University, Istanbul, 34427, Turkey

ARTICLE INFO

Keywords:
Drying shrinkage
Crack
Machine learning
Hyperparameter optimization

ABSTRACT

Concrete is a material that loses water and changes shape while hardening due to its structure. Over time, this water loss results in some shrinkage of the hardened concrete, referred to as drying shrinkage. In addition, water loss of concrete also causes the formation of various cracks. The aggregate used in concrete plays an important role in the shrinkage and cracking of concrete. The focus of this study is to accurately estimate the amount of crack width and drying shrinkage over time after the substitution of fine aggregates with other types of aggregates (consisting of various industrial by-products or wastes at different percentages) in the concrete mortar. For this purpose, various experimental results of the 'substituted fine aggregate concrete mortars' were converted into a data set. Following this a model was developed to predict the drying shrinkage and crack width of concrete mortars. The machine learning model was trained with the measurement results of 60-day drying shrinkage and crack widths of concrete mortars with different proportions of bottom ash (BA), granulated blast furnace slag (GBFS), fly ash (FA), and crushed tiles (CT). To enhance the detection/prediction capability of the model, the model hyperparameters were optimized. It is observed that the developed model was able to detect the drying shrinkage and crack width with an accuracy exceeding 99.6 %. In addition, the physical properties such as grain shape (angular or round) of components like fine aggregates may be effective for improved performance of the machine learning models in predictions of the drying shrinkage values or drying shrinkage cracking widths.

1. Introduction

In reinforced concrete structures, the durability of concrete has major impacts on strength and stability of the structure, in protection from corrosion for steel reinforcements, and in service life and overall performance of the structure. One of the key components that has a big impact on the durability of the concrete is the type of aggregate used in the concrete mortar. Along with the developments in the production industries, waste production has also increased to elevated levels, and researches have focused on consumption of the industrial wastes through recycling them into useful raw materials and products for other industries. In this context, in the construction industry, the use of industrial wastes as aggregates in concrete mortars has increased significantly. Drying

* Corresponding author.
E-mail addresses: aylaocak@outlook.com (A. Ocak), bekdas@iuc.edu.tr (G. Bekdaş), umit.isikdag@msgsu.edu.tr (Ü. Işıkdağ), melihnig@iuc.edu.tr (S.M. Nigdeli), tbilir@iuc.edu.tr (T. Bilir).

https://doi.org/10.1016/j.jobe.2024.110737
Received 13 May 2024; Received in revised form 26 August 2024; Accepted 11 September 2024
Available online 13 September 2024

shrinkage and cracks that occur as a result of drying of concrete are highly affected by the contents of the aggregate. Until recent years, usually, laboratory experiments have been carried out to observe and record the drying shrinkage and widths of cracks in concrete mortars with different compositions of aggregates. In fact, in recent years thanks to the developments in Artificial Intelligence and Machine Learning, the results of the previous experiments can be used to develop models that can successfully and accurately estimate these artifacts without the need to conduct new experiments for every new case. This innovative approach is very time and cost efficient when compared with the previous one. In this sense, in recent years there have been many studies on utilization of supervised machine learning for this purpose. In this scope, this study focused on the prediction of the crack width and drying shrinkage when alternative aggregates such as waste or industrial products replace fine aggregates in concrete mortars. Experimental methods allow testing a limited number of products by human hands and require a significant amount of time and cost. However, today's technology makes it much easier to generate new information by using already available experimental test data. For instance, the dataset used in the study is formed based on the experimental studies carried out in Bilir [1] and includes several chemical properties of fine aggregate concrete mortars consisting of, granulated blast furnace slag (GBFS), fly ash (FA), bottom ash (BA), and crushed tiles (CT) along with the measurements of crack widths and drying in concrete when these four aggregates were used in different replacement ratios of fine aggregates. Based on this dataset, in our study, a set of supervised machine learning models were trained and evaluated. The results have demonstrated that machine learning models can be very efficient in estimation of the crack width and drying shrinkage, and hyperparameter optimization contribute to the increase of overall efficiency of the model.

2. Literature review

Concrete is a building material that contains water, aggregate, and cement as the main material and stands out with its durability. Water-cement ratio, aggregate type, and the type of cement (acting as a hydraulic binder) have a big impact on ensuring the durability of the concrete. Various methods have been developed to improve the factors affecting the strength of concrete mortars. One of these is the diversification of coarse and fine aggregates used in the concrete mortar. Today, in addition to natural aggregates such as stone, sand, gravel, volcanic ash, soil, and similar substances, industrial products and wastes such as granulated blast furnace slag, fly ash, and silica fume have started to be used as concrete aggregates. In addition, researchers aim to increase aggregate options and ensure sustainability by grinding various resources in nature and evaluating resources such as waste tires, glass, ceramics, tiles, and recycled aggregates. Research on the impacts of aggregates in concrete mortars has generally focused on strength, workability, and sustainability. In the last 20 years, with the increase in mechanization and industrial products, the use of industrial wastes as aggregate types has also increased, and studies were carried out on the consumption of waste products to prevent environmental pollution. In addition, considering the possibility of access to raw materials, studies on various aggregate types have been the subject of many studies in the literature [2–27].

Concrete is a material that exhibits different mechanical properties according to the material properties it contains. Ratios of various aggregates, admixtures, and binder cement used in concrete mortars are the main factors that are effective in determining the properties of concrete such as workability, strength, shrinkage, and cracking. The concrete mortars produced lose the water they contain during solidification and shrink in volume, leading to shrinkage of the concrete and the formation of cracks. The formation of shrinkage cracks makes concrete open to external factors and reduces its durability and especially leads to acceleration of reinforcement corrosion [28,29]. To prevent shrinkage cracks in concrete, it is recommended to add materials such as fibers, shrinkage-reducing admixtures, polypropylene fibers, super absorbent polymers, expansive additives, and lightweight aggregates [29–39]. Drying shrinkage and cracks seen with the drying of concrete are highly affected by the contents of the concrete aggregate. The effects of different aggregates on drying shrinkage and cracks have been investigated in the literature. Studies in this field can be summarized as follows: Zielinski and Kaszynska conducted experimental research on self-compacting normal and lightweight concrete and observed better drying shrinkage in lightweight concrete compared to normal-weight concrete [40]. Güneyisi et al. found that the use of nano-silica and treated lightweight aggregates can reduce drying shrinkage by up to 23 % in lightweight aggregate concrete mortar from fly ash [41]. Lee et al. reported that the aggregate volume function was effective in drying shrinkage cracks when dune sand and crushed sand were used as fine aggregates in the concrete mortar [42]. Yu and Zhu observed that the use of small rubber in rubberized concrete mortar can increase the porosity and drying shrinkage of concrete [43]. Gong et al. investigated ceramsite concrete mortars with shrinkage reducer and polypropylene fiber material and found that they were effective in reducing drying shrinkage for both single and combined use cases [44]. Maghfouri et al. found that the use of a high proportion of palm oil shells as aggregate resulted in an effective increase in drying shrinkage [45]. Zhang et al. found that the use of fly ash as fine aggregate consistently reduced the drying shrinkage compared to conventional concrete [46]. Hung et al. observed that the addition of fly ash cenospheres as aggregate to high-strength lightweight concrete improved drying shrinkage [47]. Huynh et al. found that the use of dune sand instead of fine aggregate in concrete increased the drying shrinkage, while the addition of a portion of ground granulated blast furnace slag instead of cement improved the drying shrinkage effect [48]. Nasser et al. found that the use of solid waste incineration bottom ash in different proportions instead of natural aggregate in concrete initially increased drying shrinkage and improved autogenous shrinkage as a result of increasing moisture content [49]. Shi et al. observed that the use of iron waste powder and sand in concrete reduced drying shrinkage due to the pore refining effect of iron waste [50].

Developing technology has enabled many developments in the field of structural engineering. The most important reason for this is the development of artificial intelligence technologies. While many engineering problems today require various expertise and knowledge from humans, artificial intelligence technologies can reach this level of expertise in a very short time with data-based knowledge. Machine learning is an artificial intelligence method in which a machine is trained with a data set and given the ability to predict new data based on past training experience. The diversity of sources seen in building materials is an area where experience is

gained based on experimental observation results that require a long process. Machine learning techniques are trained with the results obtained from experiments on building materials, allowing the prediction of new information based on old experimental results. In studies on concrete using machine learning and its sub-branches, prediction of values such as creep behavior, compressive and tensile strength, carbonation depth, crack repair rate, crack width, crack propagation, crack detection, and mechanical properties have been investigated [51–63]. Some of the studies can be summarized as follows: Liang et al. created models that predict the creep behavior of concrete with ensemble machine learning algorithms and observed that predictions can be made that are compatible with the logic of parameters affecting the creep of concrete in behavior prediction [51]. Ren et al. proposed a deep fully convolutional neural network for the detection of concrete cracks, providing higher accuracy than some alternative and traditional methods for crack segmentation in tunnel monitoring [52]. Feng et al. used concrete compression test data to predict the compressive strength of concrete and developed a prediction model with an accuracy of 98 % with the Adaboost algorithm [53]. Bui et al. used an artificial neural network to predict the tensile and compressive values of high-performance concrete and created a hybrid expert system that makes effective predictions using the modified firefly algorithm for neural network weights in improving the performance of the model [54]. Asteris et al. tried the hybrid ensemble surrogate machine learning method using experimental data to predict the compressive strength of concrete and achieved higher accuracy compared to different traditional machine learning methods [55]. Behnood and Golafshani collected and used data from publications on the properties of concrete in which waste foundry sand was partially or completely used instead of fine aggregate, and developed models that estimate the mechanical properties of concrete (compressive strength, modulus of elasticity, flexural strength, splitting tensile strength) with the M5P algorithm [56]. Chaabene et al. examined various machine learning methods such as artificial neural network, support vector machine, decision trees, and evolutionary algorithms in predicting the mechanical properties of concrete, and presented the performance analysis and critical approach of the models [57]. Nunez and Nehdi used machine learning to determine the carbonation depth in concrete containing various mineral additives such as metakaolin, silica fume, and fly ash and using recycled aggregate, and determined that the gradient boost regression tree model showed a good prediction performance [58]. Liu et al. created a model using artificial neural networks (ANN) to predict the carbonation depth of recycled aggregate concrete, tried a hybrid method by optimizing the ANN with various swarm intelligence algorithms, and achieved a better performance than the independent artificial neural network [59]. Lou et al. used machine learning methods in self-healing concrete to create models that predict the repair rate of cracked parts in concrete and compared the performance of the methods used [60]. Yuan et al. developed machine learning models to investigate the effect of various parameters on the self-healing ability of cementitious composites, evaluated the models using Shapley additive annotation (SHAP), and observed that the crack width before healing has a significant effect on the prediction of the width after healing and that additional parameters can be used in healing prediction [61]. Dorafshan et al. investigated the performance of edge detectors in image-based crack detection of concrete structures and proposed a hybrid method in which deep convolutional neural networks and edge detectors were used together [62]. Bayar and Bilir used the machine learning method to create images of cracks in concrete and predicted the crack geometry, crack direction and propagation with the Voronoi diagrams they obtained [63]. In this study, 60-day experimental results of concrete produced by replacing the fine aggregates used in the concrete mortar with granulated blast furnace slag (GBFS), fly ash (FA), bottom ash (BA), and crushed tiles (CT) at different ratios were taken and used in machine learning training and an artificial intelligence model was developed to predict the drying shrinkage and crack width of concrete together. For this purpose, the results of the experimental study conducted by Bilir [1] were converted into a data set. Mortar samples were taken from the obtained concrete mortars and their tensile and compressive strengths were tested in 28 days of flexure [1]. The ring test was applied for free drying shrinkage for 60 days and the resulting crack widths were measured with an optical crack microscope. The following section elaborates on the dataset prepared based on Bilir [1] and model development and evaluation strategies applied for the estimation of drying shrinkage and crack widths.

3. Methodology

The methodology implemented in this research involved two stages, i.) testing of several machine learning algorithms for estimation of drying shrinkage and crack width of concrete, and ii.) hyperparameter optimization of the best-performing algorithm to achieve even better accuracy rates in estimation. In this section, a general overview of machine learning is presented, several machine learning algorithms used in the study are summarized, and the hyperparameter optimization concept is explained briefly.

3.1. Machine learning

Artificial Intelligence (AI) refers to the ability of machines, a computer, and software with a similar function, to create decision-making mechanisms that mimic the human brain. Machine learning is a type of artificial intelligence that allows machines to make inferences by training them with data. It offers two types of inference goals. The machine learning model can perform classification as well as numerical predictions expressed as regression problems [64,65]. When faced with a classification problem, the machine classifies the data into certain categories/classes according to the characteristics of these classes. For regression problems, machine learning makes it possible to establish a numerical relationship between the inputs and outputs of the data, and the inferential model it develops can make numerical predictions for the new inputs. Machine learning is divided into various sub-branches. In broad terms, these are as follows: Supervised learning is a branch of machine learning in which inputs and outputs are used to train the machine and the machine can predict the outputs for each new input with the knowledge gained. Unsupervised learning aims to predict the outcome (i.e. categories of data) without the outputs in a data set, by searching for a relationship between the inputs to each other. In other words, unsupervised learning seeks an order among inputs [66]. Deep learning is a machine learning method that mimics the human brain with multi-layer neural networks using large amounts of data [69].

Reinforcement learning is another branch of AI that acts on actions and targets new actions based on previous actions, as seen in

robotic technology [64,67]. An example of reinforcement learning is when a telephone user changes his/her location to get a better signal and does not have any information about the new location and does not choose the locations where he/she finds the phone signal bad according to his/her previous experiences [68]. Here, the user aims to obtain the correct location by performing a kind of mapping process for the location with negative results.

3.2. Regression algorithms

Regression is a machine learning method, successfully implemented in statistics for many years, for establishing a connection between dependent variables(outputs) and independent variables(inputs) in data. Most well-known regression methods include linear regression for the estimation of numerical dependent variables, and logistic regression for the estimation of categorical dependent variables. In most cases, in machine learning models developed with regression algorithms, the effect and relationship of inputs on outputs can be analyzed and the output of each new input can be numerically predicted. In regression problems, besides foundation algorithms such as linear, nearest neighbor, and decision tree, ensemble algorithms such as Adaboost, Lightgbm, Catboost, Xgboost, and Bagging can also be used. The algorithms used in this study are briefly described below.

Decision Tree: Decision Tree Regressor builds a tree-like structure based on the attributes in the data and the predictions corresponding to these values, called nodes. The tree continues to grow according to a predefined stopping criterion from the terminal nodes to the root node, which is reached with the best prediction. This structure of leaves, branches, and roots is easy to understand and makes it easy to find the relationship between a normal variable and a high-impact variable [70–72].

K-Nearest Neighbors: K-Nearest Neighbors Regressor is a machine learning algorithm that aims to find K instances in a data set that are the closest distance from a random sample [73]. The performance of this algorithm is related to the setting of the value of K, the number of nearest neighbors. The distance between the samples is set by the optimal choice of the value of K and the weight vector [74].

Lasso: Lasso Regressor is an algorithm that aims to obtain a good predictor even for rare features by minimizing the values in the data [75]. This minimization is intended to reduce the complexity of the data and is functional in models with many attributes as input. It deals with the elimination of some features to avoid overfitting [76].

Ridge: Ridge Regressor is a method used to eliminate multicollinearity when there is a high correlation between two or more independent variables in the data. It identifies the attributes that have little effect on the data and reduces their coefficients [76]. In regression analysis, it aims to reduce standard errors by taking deviations into account [77].

ElasticNet**:** ElasticNet regressor is a machine learning algorithm that aims to reduce the sum of errors. It is a regressor that combines the two methods by taking the coefficients of the equations used in the lasso and ridge regressors. In its simplest form, it combines the lasso algorithm's method of removing low-impact features and the ridge algorithm's method of reducing the coefficients of insignificant features [76].

Linear Regression**:** Linear regression is a machine learning algorithm that aims to establish a linear relationship between dependent and independent variables. In its basic logic, the output values to be predicted are considered as a linear line, and a linear relationship is established between inputs and outputs by adding weights to the inputs in the data. While the output values (y's), which are dependent variables, are expected to be continuous, the input values (x's), which are independent variables, can be continuous or discrete [78, 79**] .**

Bagging**:** A bagging regressor is a machine learning method that multiplies the dataset by adding more training data to produce a prediction model and determines the final ensemble prediction by averaging the individual predictions. It is stated that it is a powerful algorithm for solving problems arising from overfitting, increasing prediction success and data variability in regression problems [80].

Random Forest**:** It is an ensemble algorithm that creates decision trees using randomly selected feature subsets in the data and obtains results by averaging the predictions. One of the main problems of decision tree algorithms is overfitting. To keep this situation under control and produce a more accurate prediction, bootstrapped samples, decision trees, and randomly selected data features are used [79,81].

AdaBoost**:** The AdaBoost (Adaptive Boosting) algorithm is essentially an ensemble algorithm that aims to produce a stronger model by bringing weak students together. Equal weights are given to the initially trained data points. Later, the performance of the model can be improved by updating and adjusting these weights according to incorrect predictions [78].

XGBoost**:** It is a gradient boosting algorithm called extreme gradient boosting, which is a more advanced version of the gradient boosting algorithm based on ensemble learning [82]. It is advantageous compared to other algorithms in terms of feature selection and convergence speed [83].

LightGBM: The LightGBM algorithm is a machine learning method for gradient boosting, called light gradient boosting machine. It was developed by using exclusive feature bundling and gradient-based one-side sampling methods together [84,85]. It has outstanding advantages over other algorithms in issues such as missing data, distributed computing, and parallelism [86].

CatBoost: It is a machine-learning algorithm developed for enhancing gradient boosting [87,88]. Overfitting, which is usually seen in gradient boosting algorithms, is an issue that can be overcome in this algorithm. Compared to similar gradient boosting algorithms such as LightGBM and XGBoost, it overcomes the overfitting problem thanks to its training speed and solves target leakage with sequential boosting [89].

3.3. Hyperparameter optimization

Machine learning algorithms have different mechanisms that express the relationship between the dependent and independent variables in data. The coefficients of the functions in these represent the model parameters. During machine learning, model parameters are optimized to increase performance by using various optimization techniques. Unlike model parameters, hyperparameter

is a term that refers to the various characteristics of machine training, such as the process and speed of training, which are determined before machine training. By optimizing the hyperparameters, overfitting and underfitting situations can be overcome and the accuracy performance of the machine learning prediction model can be increased. There are various optimization methods and tools for hyperparameter optimization. Optuna is one of the well-recognized hyperparameter optimization tools developed for this purpose [90] and is implemented in our study. The flowchart of prediction model generation with the CatBoost algorithm and Optuna for the concrete data set used in the study is given in Fig. 1.

3.4. Model metrics

Machine learning algorithms cannot be clearly distinguished as better or worse than each other. Depending on the type of problem and the characteristics of the data, the algorithm that provides high accuracy in machine learning may vary. Therefore, it is necessary to test as many algorithms as possible to achieve a good model performance. The R-squared value is used as a measure of success in

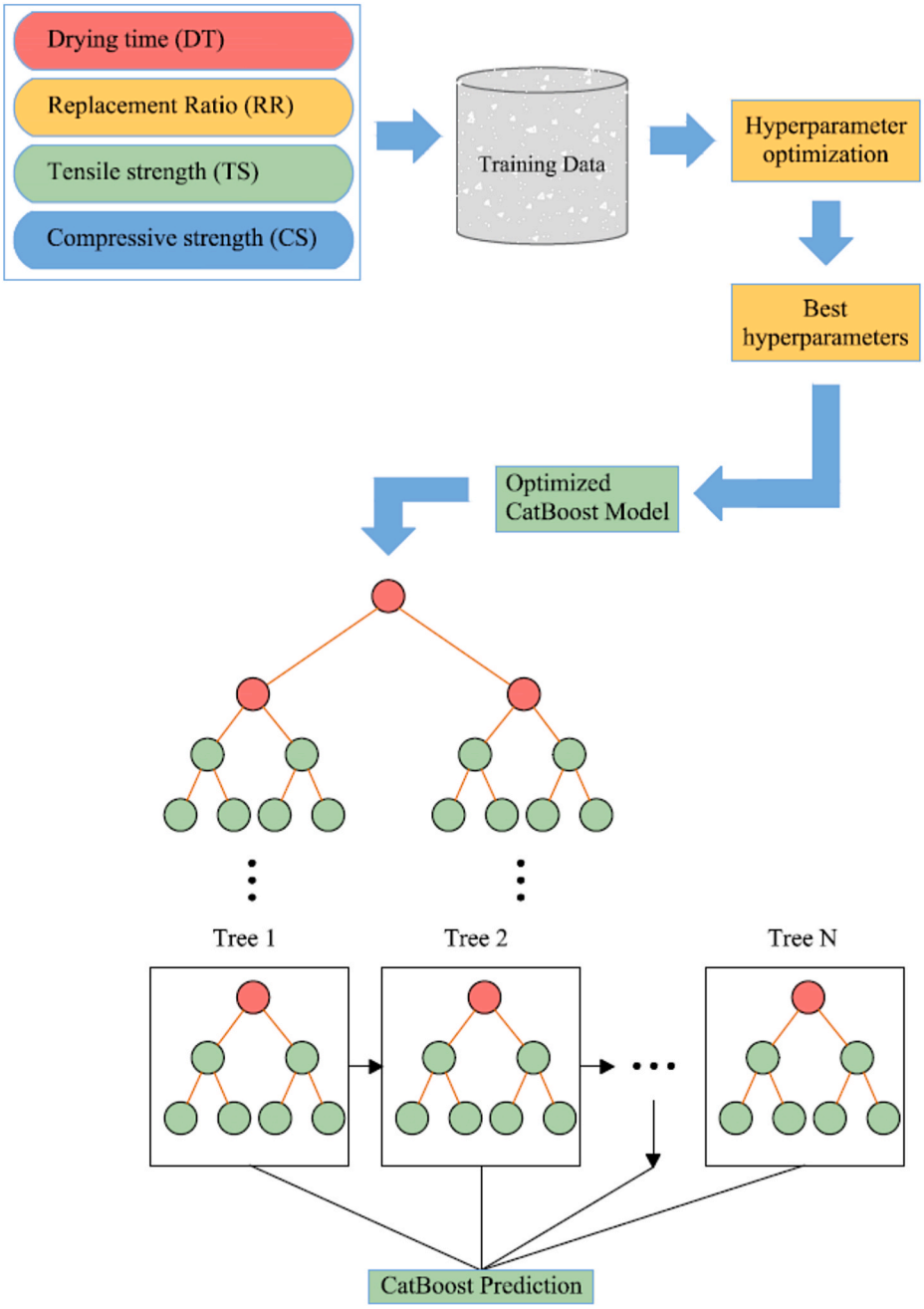

Fig. 1. Optimized CatBoost Model flowchart for training data.

regression models. This value, expressed as the variability ratio of the regression, symbolizes the power of regression analysis and shows how much the total variation in the machine learning model can be explained. In regression problems, besides the R-squared value, values such as Mean Squared Error (MSE), root mean square error (RMSE) and mean absolute error (MAE) are also helpful metrics in interpreting the regression problem. The calculation of, R-squared (R^2) is shown in Equation (1), mean absolute error (MAE) is shown in Equation (2), mean square error (MSE) is shown in Equation (3), and root mean square error (RMSE) is provided in Equation (4).

$$R^2 = 1 - \frac{\sum_{i=1}^{N} (y_i - \hat{y}_i)^2}{\sum_{i=1}^{N} (y_i - \bar{y}_i)^2} \tag{1}$$

$$MAE = \frac{1}{N} \sum_{i=1}^{N} |\hat{y}_i - y_i| \tag{2}$$

$$MSE = \frac{1}{N} \sum_{i=1}^{N} (\hat{y}_i - y_i)^2 \tag{3}$$

$$RMSE = \sqrt{\frac{1}{N} \sum_{i=1}^{N} (\hat{y}_i - y_i)^2} \tag{4}$$

In the equations, the number of samples is denoted as N, and the observation value and their mean are denoted by y_i and $\bar{y}_i$, respectively, and the predicted value is denoted by $\hat{y}_i$.

3.5. Model evaluation

Different methods are used to validate machine learning models. In this study, we used the k-fold cross-validation method proposed by Geisser and Eddy [91,92], which is based on the principle of sample reusability and has a simple and straightforward structure. This method divides the data into k parts and uses k-1 parts as training data, while each part is used for validation. For the models to be used in the study, the data is divided into 10 folds and each fold is used separately as validation data. The remaining 9 pieces out of each fold are taken as training data for the model. The process is performed 10 times in total for all folds and 10 different R-squared values are obtained. The accuracy of the model is determined by taking the average R-squared value of 10 folds. A visual summary of the k-fold cross-validation method is shown in Fig. 2.

4. Results

In this study, a machine learning model was developed for a dataset consisting of the fine aggregates' replacement ratios of concrete mortars with different aggregates, drying time, average tensile and compressive strengths, drying shrinkage, and crack widths. In the developed model, various regression algorithms were tested to define a model that predicts drying shrinkage and crack width at the same time.

4.1. Dataset and Exploratory data analysis

Various properties of fine aggregate concrete mortars consisting of granulated blast furnace slag (GBFS), fly ash (FA), bottom ash (BA), and crushed tiles (CT), of which experimental studies were carried out by Bilir [1], were used in this study. In his study [1], Bilir recorded the crack widths and drying shrinkage that would occur in concrete if these four aggregates were added to the concrete

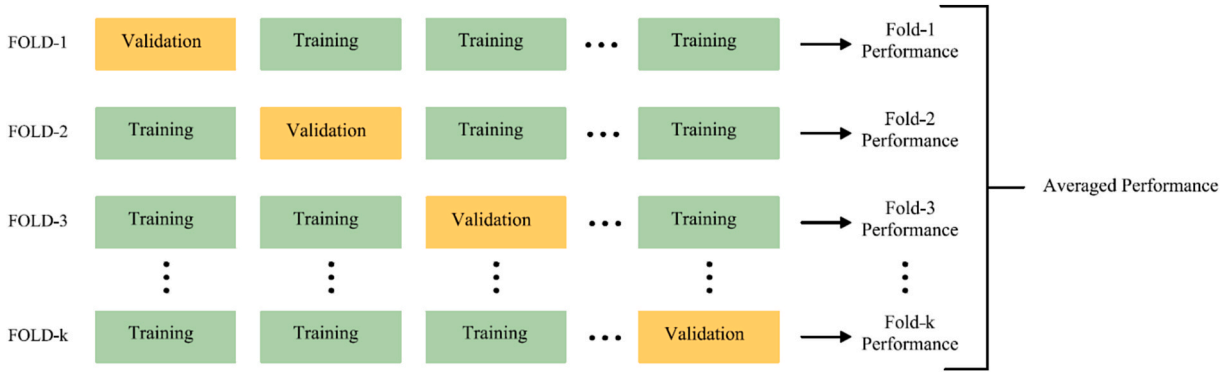

Fig. 2. K-fold cross-validation method.

mortars in different replacement ratios of fine aggregate, with experimental measurements and observations for a period of 60 days. In the data, 60-day drying shrinkage obtained by applying the ring test to Portland cement mixtures, average crack widths measured according to drying time, and 28-day average tensile and compressive strengths determined according to addition rates were used. The physical and chemical properties of the aggregate types used in the study are shown in Tables 1 and 2, respectively.

The data consisted of 2640 lines. The characteristics of the data is summarized in Table 3. A sample of 11 lines of the data used in the study is provided in Table 4. The correlation matrix of the data set is given in Table 5 and the correlation chart is shown in Fig. 3.

4.2. Evaluation of machine learning (ML) algorithms

In our study, a machine learning model that predicts drying shrinkage and crack width together from the concrete data set consisting entirely of numerical data was developed. In the model generation process, the popular machine learning algorithms of the Scikit-Learn package [93], along with some other ML packages were evaluated using 10-fold cross-validation, and the model with the highest accuracy (R-squared score) was then retrained for hyperparameter optimization with Optuna. The calculated performance indices of the algorithms tested in the data set prior to hyperparameter optimization are given in Table 6. The table includes the highest R-squared score among 10-folds (Max-R2), the average of R-squared scores of 10-folds (Mean-R2), average mean absolute error (MAE), mean squared Error (MSE) and root mean square error (RMSE) values.

Considering the R-squared values given in Table 6, hyperparameter optimization was applied to the best-performing algorithm, CatBoost. In this study, Optuna Hyperparameter Optimization is used for optimizing the hyperparameters of the CatBoost algorithm. The hyperparameters (and their definitions) used in the optimization process are provided in Table 7.

The optimum values of the hyperparameters, the new mean R-squared value of 10-folds after hyperparameter optimization, and the maximum R-square value at which the highest value was obtained among the folds are given in Table 8. Although the achieved accuracy with CatBoost was very high, it is observed that the mean accuracy rate can be further enhanced through hyperparameter optimization.

5. Discussion

In this study, the machine learning model was developed using a data set of experimental measurements of various concrete mortars to accurately estimate the drying shrinkage and crack width. For this purpose, 60-day measurement data of concrete specimens produced by adding different proportions of fine aggregates consisting of granulated blast furnace slag (GBFS), bottom ash (BA), fly ash (FA), and crushed tiles (CT) to concrete mortars along with obtained drying shrinkage and crack width is used for supervised machine learning training. In the model, the drying time, average tensile and compressive strengths of the concrete specimens, and the addition rates of the fine aggregate in the concrete mortars at 10 % increments between 0 and 100 % were used as the input data. The developed model jointly predicts the drying shrinkage and crack width of concrete specimens. In developing the model, 12 different regression algorithms were tested (Table 6) and the highest accuracy was observed for the CatBoost regressor with a mean R-squared value of 0.9959. Mean absolute error (MAE), mean squared error (MSE), root mean squared error (RMSE), and mean R-squared error (mean-R2) scores of the algorithms used in the study were calculated as comparison metrics. These MAE, MSE, and mean R-squared scores are presented in Figs. 4-6, respectively.

As shown in the MAE values in Fig. 4, it can be seen that the lowest value was obtained with the Bagging and XGBoost models. The mean absolute error values were very close and low, especially in the ensemble algorithms, except for the AdaBoost model. Adaboost algorithm works on determining the correct weight coefficients to strengthen weak students in education. In the Adaboost model, since the data points were initially given equal weights and these weights were updated according to incorrect predictions, the mean absolute error value was higher compared to other composite algorithms. Models in which the error rates were close to each other and had low absolute errors belonged to Decision Tree, LightGBM, Bagging, Random Forest, XGBoost, and CatBoost algorithms.

According to the MSE values in Fig. 5, the lowest MSE value was observed for the model trained with the CatBoost and XGboost algorithms. Among the models trained with XGboost and Bagging algorithms (i.e. the models with the lowest MAE values), CatBoost and XGboost have given the lowest MSE value, while the Bagging model gave the third lowest mean square error.

The CatBoost algorithm had very low MAE and MSE values. In fact, the training with XGBoost algorithm resulted in better MAE rates with a minor positive difference (i.e. lower value). The MSE values of these two algorithms were the same. However, considering the average R squared (R2) and max R2 values, CatBoost was the algorithm that provided the most accurate results. There are different points of view in the selection of the evaluation metrics for the regression models. While MAE takes the absolute value of the difference between the predicted values and the real value in the data, MSE follows a method that is more sensitive to outliers and penalizes the large errors more heavily by using the square of this difference. In addition, when there is optimization in the process MSE can be regarded as a more mathematically more convenient metric. In this sense, MSE distinguishes incorrect predictions more sensitively than MAE and can show the error more clearly and squarely. Looking at the MSE values, XgBoost and CatBoost algorithms showed the exact same error rates. The other evaluation criterion, R2 value expresses the model's adaptability to explain the data. By focusing on all 3 metrics MAE,MSE and R2 in a holistic manner, the CatBoost appears as the most accurate model. Accordingly, considering all the evaluation criteria, the CatBoost algorithm is determined as the best model.

When the mean R-squared scores in Fig. 6 are examined, it is seen that Random Forest, XGBoost, Bagging, Decision Tree, and CatBoost algorithms achieve an accuracy exceeding 99 %, which can be regarded as an excellent prediction accuracy. With hyperparameter optimization, the performance of the CatBoost regressor model, which has the highest mean R-squared score, also increased where the accuracy level (mean-R2) reached 99.66 %.

In this study, the Catboost algorithm hyperparameters were optimized and a maximum R-squared value of 0.9980 was obtained

Table 1
Fine aggregate chemical properties.

	SiO_2	Al_2O_3	Fe_2O_3	CaO	MgO	SO_3	MnO	TiO_2	P_2O_3	K_2O	Na_2O	Free Cl^-	CT	Undetermined
	(%)													
GBFS	35.09	17.54	0.70	37.79	5.50	0.66	0.83	0.68	0.37	0.60	0.30	–	–	–
FA	58.69	25.10	5.80	1.49	2.22	0.12	–	–	–	4.04	0.59	0.013	1.28	–
BA	57.90	22.60	6.50	2.00	3.20	0.60	0.09	57.90	22.60	6.50	2.00	–	–	–
CT	50.99	13.76	5.025	10.64	–	–	–	–	–	2.115	0.6	–	–	13.02

Table 2
Fine aggregate physical properties.

	GBFS	FA	BA	CT
Loose unit weight (kg/m^3)	1052	870	620	–
Compressed unit weight (kg/m^3)	1236	1110	660	–
Unit weight	2.08	1.80	1.39	1.9
Water absorption rate (%)	10	–	12.10	18
Organic material (color)	Light yellow	–	Light yellow	–
Loss on Ignition (%)	9.4	–	2.40	–
Light particles (%)	3	–	7.00	–

Table 3
Descriptive statistics of the dataset.

Feature	Drying Time	Replacement Ratio	Tensile Strength	Compressive Strength	Drying Shrinkage	Crack Width
	Day	%	N/mm^2	N/mm^2	–	mm
Minimum variable	1	0	1.66	12.10	0	0
Maximum variable	60	100	10.34	46.77	0.0196	2.25
Mean	30.5	50	5.023	29.56	0.0047	0.4887
Standard deviation	17.32	31.63	2.098	9.04	0.0037	0.6105
Variance	299.9	1000	4.399	81.62	1.39E-05	0.3726
25 %	15.75	20	3.408	21.46	0.0023	0
50 %	30.5	50	4.645	30.11	0.0036	0.1035
75 %	45.25	80	5.85	36.88	0.0063	0.9433

Table 4
First 11 rows of the dataset.

Drying Time (day)	**Replacement Ratio (%)**	**Tensile Strength (N/mm^2)**	**Compressive Strength (N/mm^2)**	**Drying Shrinkage**	**Crack Width (mm)**
1	0	5.41	40.27	0.000105	0
1	10	5.1	37.53	0.000235	0
1	20	4.65	32.17	7.37E-05	0
1	30	5.2	38.89	0.000277	0
1	40	5.4	41.85	0.000428	0
1	50	4.42	29.66	0.000105	0
1	60	3.61	22.60	0.000358	0
1	70	3.89	30.36	0.000267	0
1	80	3.43	27.33	0.000305	0
1	90	3.34	23.94	0.000249	0
1	100	3.19	21.46	0.000265	0

Table 5
The correlation matrix.

	Drying Time (DT)	**Replacement Ratio (RR)**	**Tensile Strength (TS)**	**Compressive Strength (CS)**	**Drying Shrinkage (DS)**	**Crack Width (CW)**
Drying Time (DT)	1	2.53E-16	−6.25 E−16	2.96 E−16	0.3065	0.6008
Replacement Ratio (RR)	2.53 E−16	1	−0.3678	−0.8756	0.2375	−0.3578
Tensile Strength (TS)	−6.25 E−16	−0.3678	1	0.2175	0.4287	0.1448
Compressive Strength (CS)	2.96 E−16	−0.8756	0.2175	1	−0.3251	0.3158
Drying Shrinkage (DS)	0.3065	0.2375	0.4287	−0.3251	1	0.3883
Crack Width (CW)	0.6008	−0.3578	0.1448	0.3158	0.3883	1

among the 10 folds of the 10-fold cross-validation model, as shown in the results in Table 8. Accordingly, the experimental values of drying shrinkage and crack widths in the fold, Graphs of experimental values, and model prediction values of drying shrinkage and crack widths according to aggregate replacement ratios for the fold where the maximum R-squared value was obtained are given below. For GBFS aggregate, drying shrinkage is shown in Fig. 7, and experimental values and model-predicted values graphs of crack widths are shown in Fig. 8. Drying shrinkage and crack width graphs of the experimental values and model-predicted values of the same aggregate according to drying times are given in Figs. 9 and 10, respectively.

When Figs. 7 and 8 are examined, it is seen that the developed optimized model generates predictions that almost overlap with the

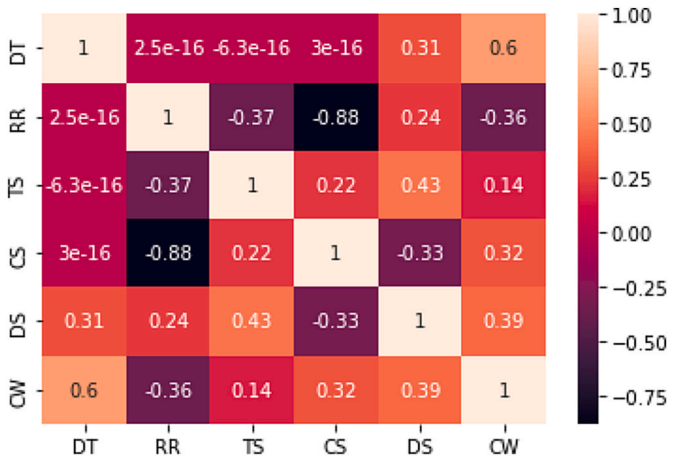

Fig. 3. The correlation chart.

Table 6
R-squared scores of regression algorithms for the sample data set.

Regressor Algorithm	MAE	MSE	RMSE	Max-R2	Mean-R2
Lasso	0.1700	0.0975	0.2224	0.2560	0.2365
ElasticNet	0.1686	0.0960	0.2206	0.2568	0.2398
Ridge	0.1684	0.0955	0.2194	0.5206	0.4733
Linear Regression	0.1684	0.0954	0.2197	0.4992	0.4782
AdaBoost	0.1285	0.0518	0.1570	0.8098	0.7654
K-Nearest Neighbors	0.0447	0.0302	0.1261	0.9190	0.8810
LightGBM	0.0137	0.0025	0.0335	0.9944	0.9896
XGBoost	0.0079	0.0011	0.0232	0.9945	0.9913
Decision Tree	0.0087	0.0032	0.0332	0.9942	0.9917
Bagging	0.0079	0.0022	0.0292	0.9970	0.9932
Random Forest	0.0080	0.0016	0.0267	0.9981	0.9946
CatBoost	0.0093	0.0011	0.0242	0.9982	0.9959

Table 7
CatBoost Regressor Algorithm hyperparameters [94].

Hyperparameter	Definition
depth	Optimum depth limit of the decision tree
learning_rate	Learning rate used to reduce gradient step
iterations	Maximum number of trees
l2_leaf_reg	L2 regularization coefficient
random_strength	Amount of randomness
bagging_temperature	Bayesian bootstrapping adjustment
border_count	Division number limit for numerical properties

Table 8
Optimum CatBoost Algorithm hyperparameters and new R-squared value.

Hyperparameter	**Optimum values**
Depth	10
learning_rate	0.1724
iterations	1000
l2_leaf_reg	0.8574
random_strength	1.5011
bagging_temperature	0.2624
border_count	236
New Mean R-squared value	0.9966
Max R-squared value	0.9980

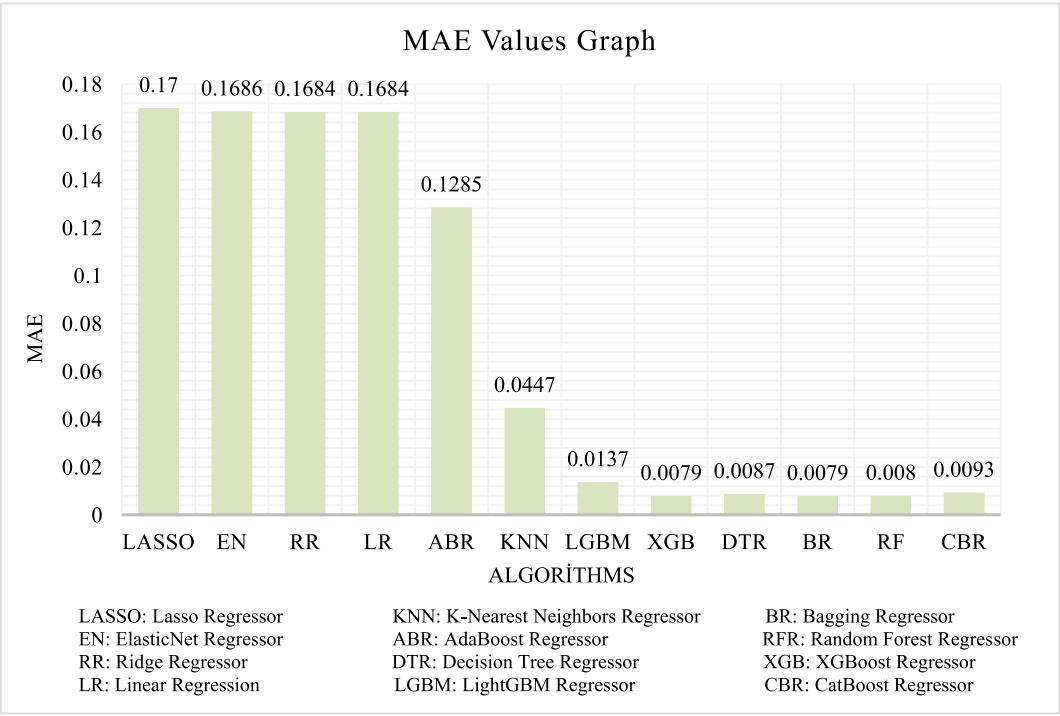

Fig. 4. Graph of MAE values of algorithms.

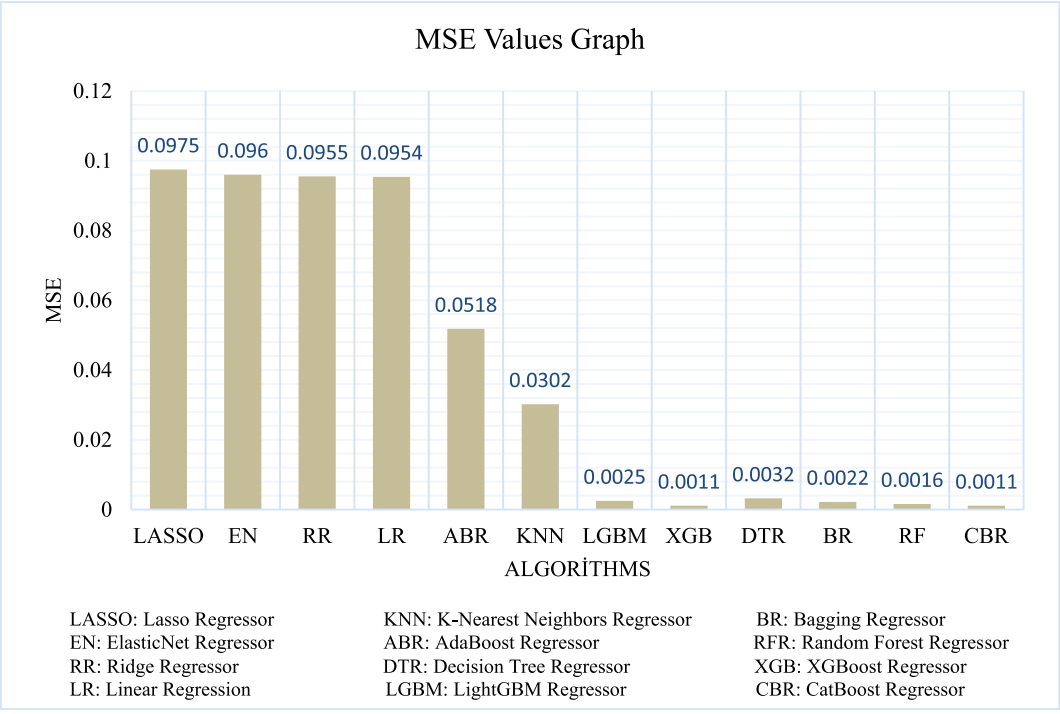

Fig. 5. Graph of MSE values of algorithms.

experimental values for drying shrinkage and crack widths depending on the replacement rate of GBFS aggregate. The crack width-replacement ratio graph showed that the predicted values were closer to the experimental values than the drying shrinkage-replacement ratio graph. This situation was also observed in the estimated values of drying shrinkage and crack widths based on

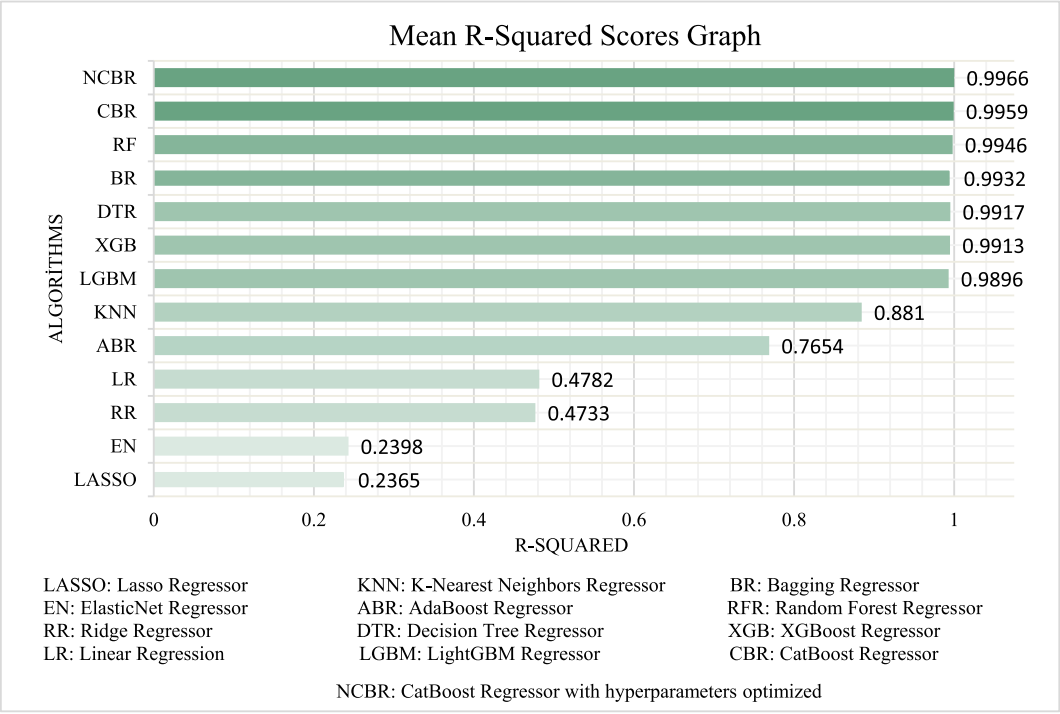

Fig. 6. Graph of R-Squared values of algorithms.

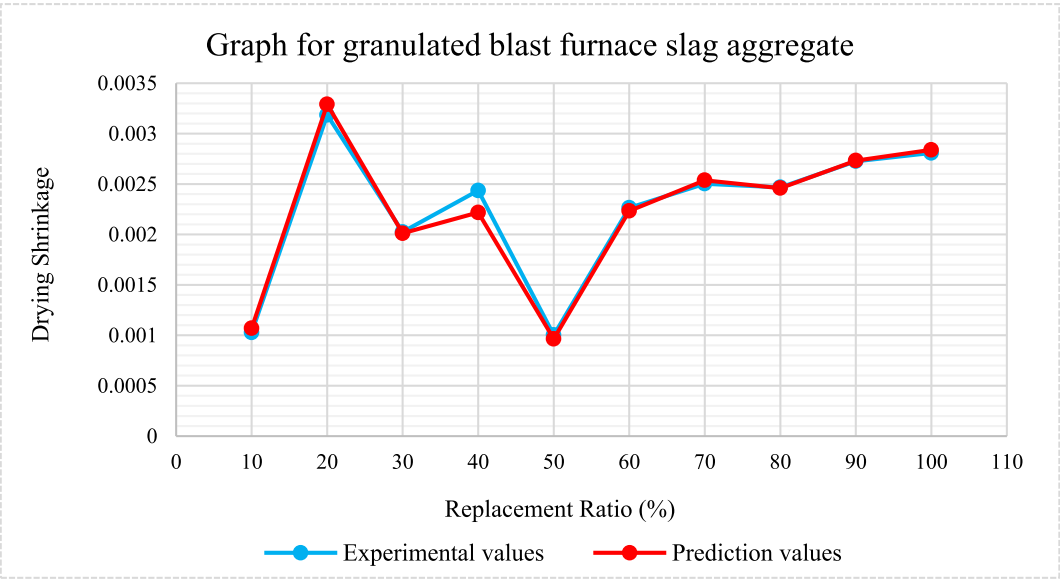

Fig. 7. Model prediction value and experimental value graph for drying shrinkage of GBFS aggregate based on replacement ratio.

drying time in Figs. 9 and 10. According to this, it can be said that the prediction consistency of the model created for GBFS aggregate may be more effective in predicting crack width compared to drying shrinkage.

The experimental value and predicted value graphs according to 10 randomly selected different replacement ratios of the BA aggregate in the fold where the highest R-squared score was obtained among the 10folds are shown in, Fig. 11 for drying shrinkage and in Fig. 12 for crack width. Drying shrinkage and crack width graphs drawn according to drying times are shown in Figs. 13 and 14, respectively.

When Figs. 11 and 12 are examined, it is seen that the values predicted by the model for BA aggregate are very close to the experimental values. According to the graphs, depending on the aggregate replacement rate, the model predicted the crack widths

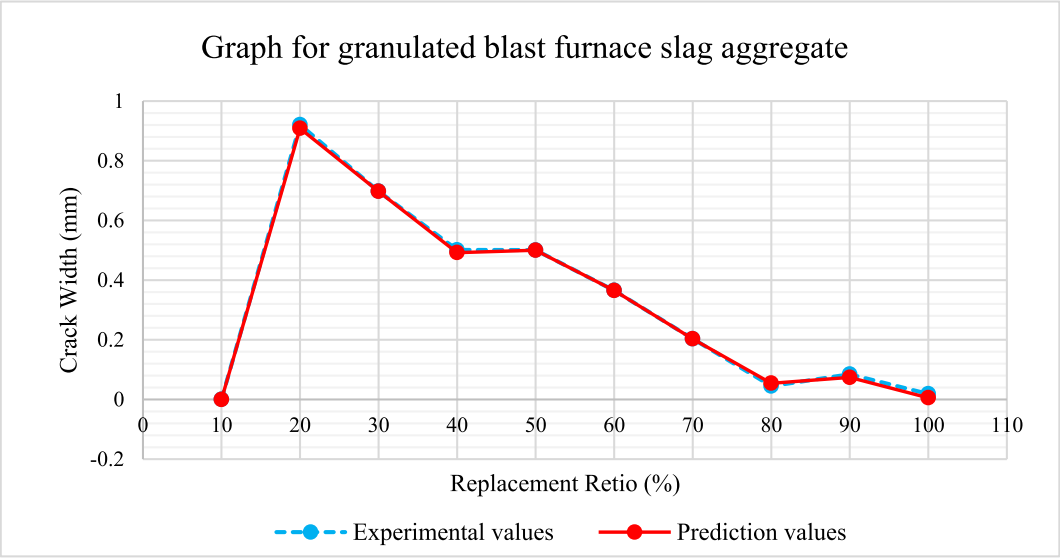

Fig. 8. Model prediction value and experimental value graph for crack width of GBFS aggregate based on replacement ratio.

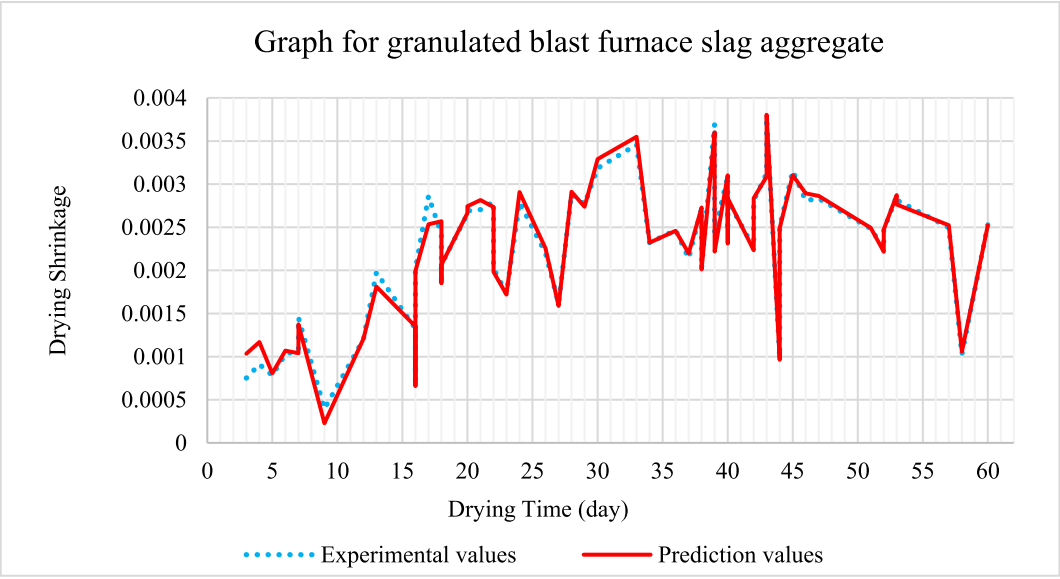

Fig. 9. Model prediction value and experimental value graph for drying shrinkage of GBFS aggregate based on drying time.

much more closely than the drying shrinkage. When the shrinkage and crack width graphs according to drying time are examined, it is seen that the experimental values and the predicted values progress in the same direction and the values overlap.

Drying shrinkage and crack width prediction graphs were obtained for different replacement rates, regardless of the drying time of the CT aggregate in the fold with the maximum R-squared value of the optimized model. The drying shrinkage-replacement ratio graphs are given in Fig. 15 and the crack width-replacement ratio graphs are given in Fig. 16, which contain the experimental values and predicted values for the CT aggregate. The drying shrinkage-drying time graph for CT aggregate, where different aggregate replacement rates are taken according to the drying time, is shown in Fig. 17 and the crack width-drying time graph is shown in Fig. 18.

When Figs. 15 and 16 are examined, it is observed that the drying shrinkage predictions for the CT aggregate tend close to the experimental values compared to the crack width prediction performance. This is valid for random percentages among the CT aggregate data within a fold selected from the maximum of all data. However, when Figs. 17 and 18 were examined, it is seen that in the graph where drying time is considered and there are many replacement ratios, the drying shrinkage prediction values are estimated almost in the same line with the experimental values, while there are small differences in the crack width prediction. Taking this into consideration, it can be said that the model may be more effective in predicting drying shrinkage for CT aggregate compared to crack

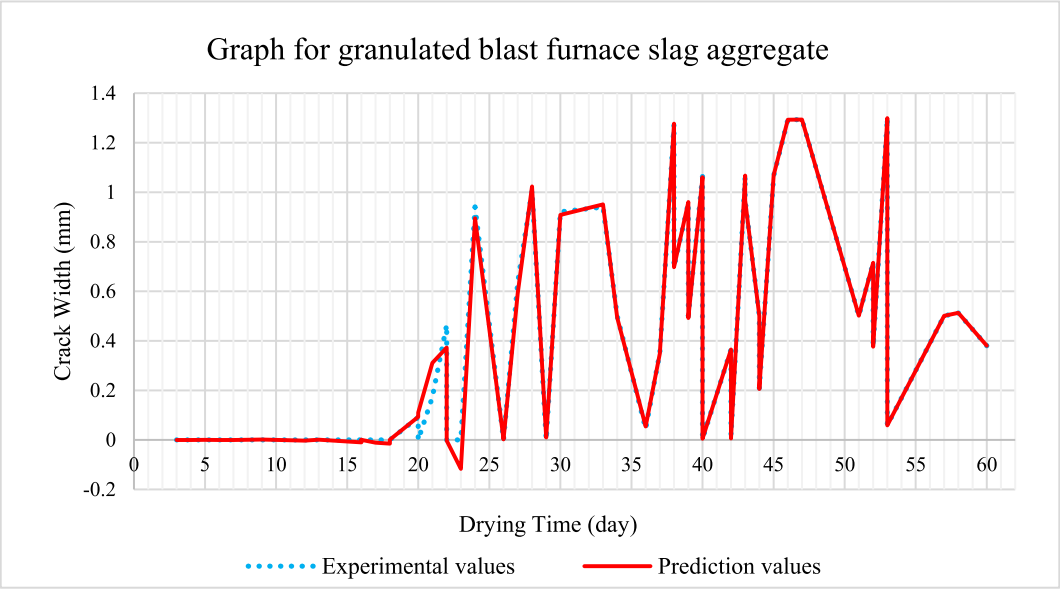

Fig. 10. Model prediction value and experimental value graph for crack width of GBFS aggregate based on drying time.

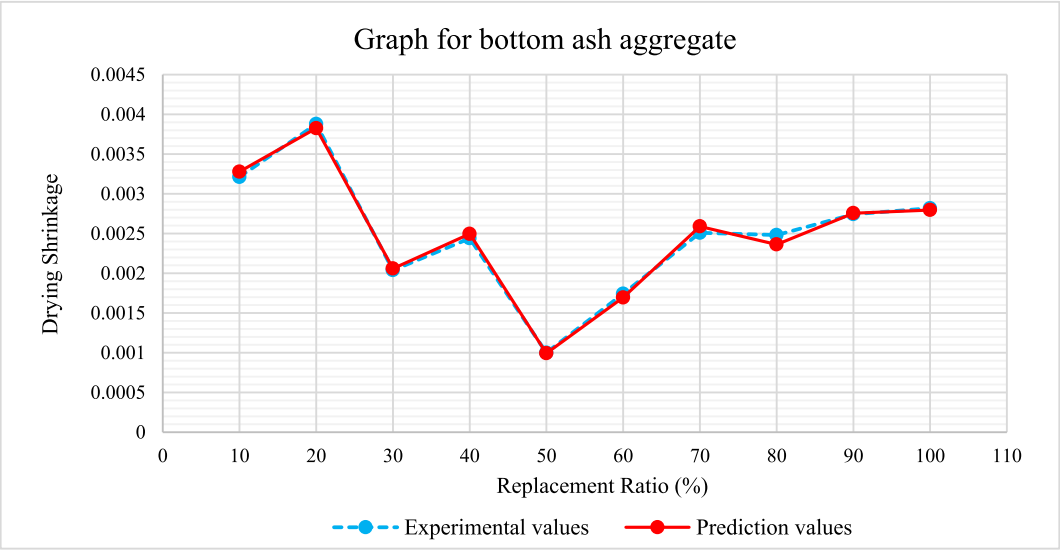

Fig. 11. Model prediction value and experimental value graph for drying shrinkage of BA aggregate based on replacement ratio.

width.

Graphs of ten different aggregate replacement ratios randomly taken from the data of the FA aggregate in the fold with maximum R-squared value for the optimized model are presented below. The drying shrinkage-replacement graph of the model-predicted and experimental values of the FA aggregate, independent of the drying time and depending on the replacement rate, is given in Fig. 19 and the crack width-replacement graph is given in Fig. 20. Taking into account the drying time, the drying shrinkage and crack width graphs of all FA aggregate prediction values in the fold are given in Figs. 21 and 22, respectively.

When the prediction graphs made with FA aggregate are examined, it is seen that the model is more effective in predicting drying shrinkage compared to the crack width prediction results.

According to the findings, it is seen that the model is more effective in predicting the drying shrinkage for GBFS and BA aggregates and the crack widths for CT and FA aggregates in the graphs based on the aggregate replacement rate. These results can be considered as interesting outcomes. The reason is that GBFS and BA are relatively more angular-shaped aggregates compared to CT and FA. CT and FA shapes can be said as round or more round compared to GBFS and BA. In this manner, it is an interesting result that aggregate shape can affect the performance of the developed model like the one of our study that CBR and optimized CBR (NCBR) can predict the drying

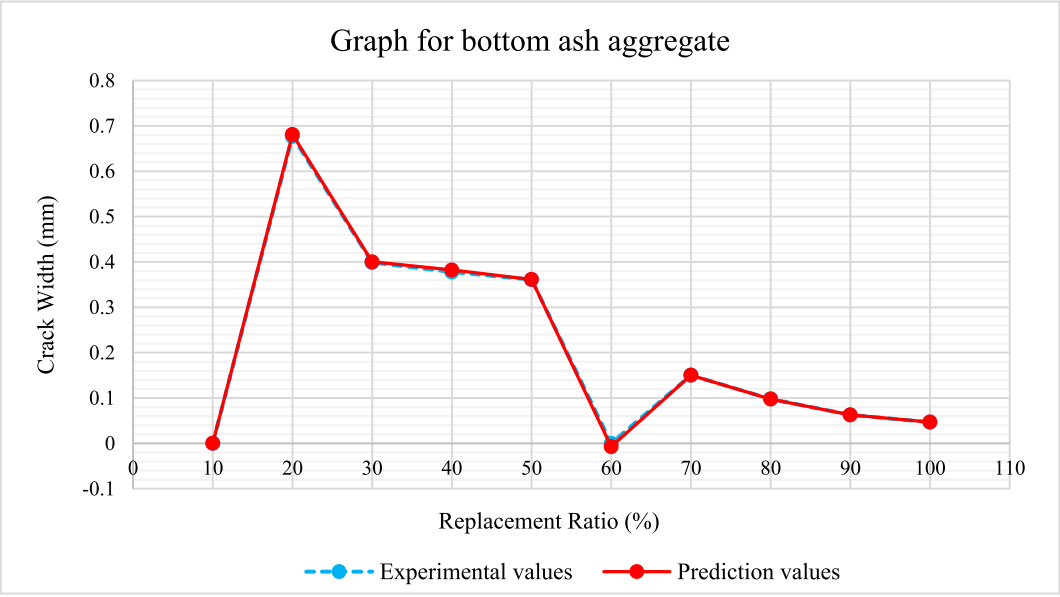

Fig. 12. Model prediction value and experimental value graph for crack width of BA aggregate based on replacement ratio.

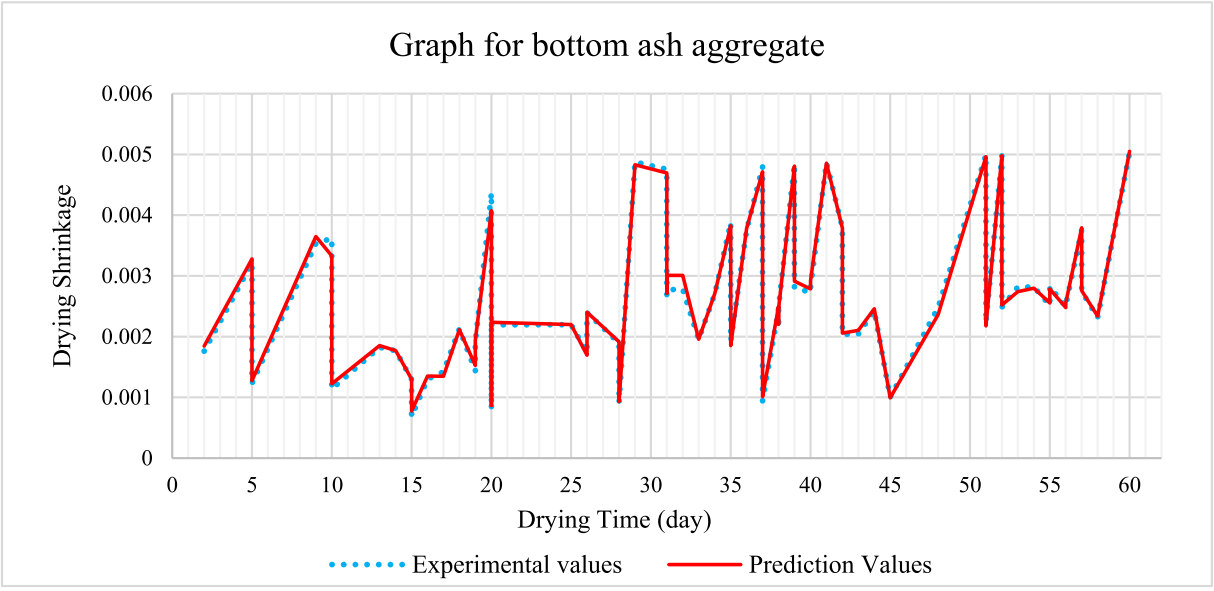

Fig. 13. Model prediction value and experimental value graph for drying shrinkage of BA aggregate based on drying time.

shrinkage values of relatively angular-shaped aggregates better than round ones and can predict drying shrinkage cracking better for more round artificial fine aggregates compared to relatively angular ones. In other words, it is well known that the properties of mortar or concrete components such as cement, aggregates, admixtures, or mixing water can affect the mechanical, durability, and physical properties of mortar or concrete like tensile and compressive strengths, unit weight, modulus of elasticity, plastic, autogenic, carbonation, thermal or drying shrinkages and cracking along with freezing-thawing, alkali aggregate reactions, sulfate attack, etc. however, considering the performances of CBR and optimized CBR(NCBR), such properties may affect the selection of machine learning techniques or model types to estimate or predict other properties of such mortar or concrete types. Actually, such properties of fine aggregates like gradation, specific surface, aggregate surface texture and shape, modulus of elasticity-rigidity, and water absorption affect the properties like the ones presented in this study as inputs and outputs like tensile and compressive strengths, drying shrinkage, and drying shrinkage cracks experimentally at the same time. In other words, the properties of aggregates are related to both inputs such as tensile and compressive strengths, and outputs such as drying shrinkage unit deformations and drying shrinkage cracks' width input into CBR and optimized CBR (NCBR). Furthermore, the tensile and compressive strengths also are both interact or

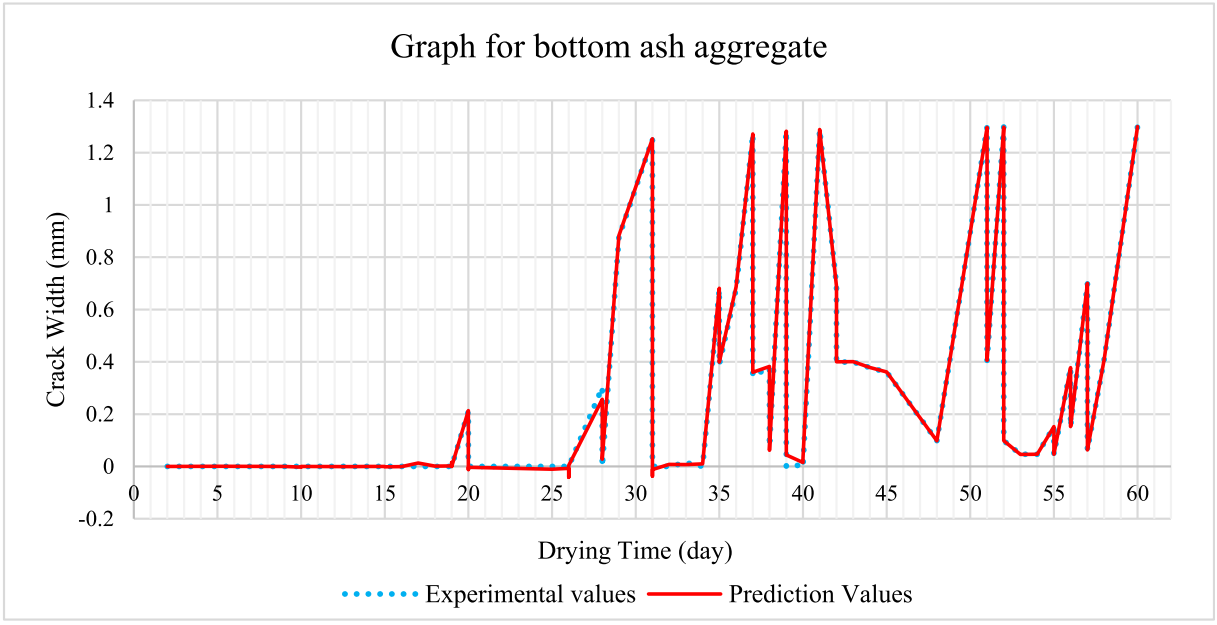

Fig. 14. Model prediction value and experimental value graph for crack width of BA aggregate based on drying time.

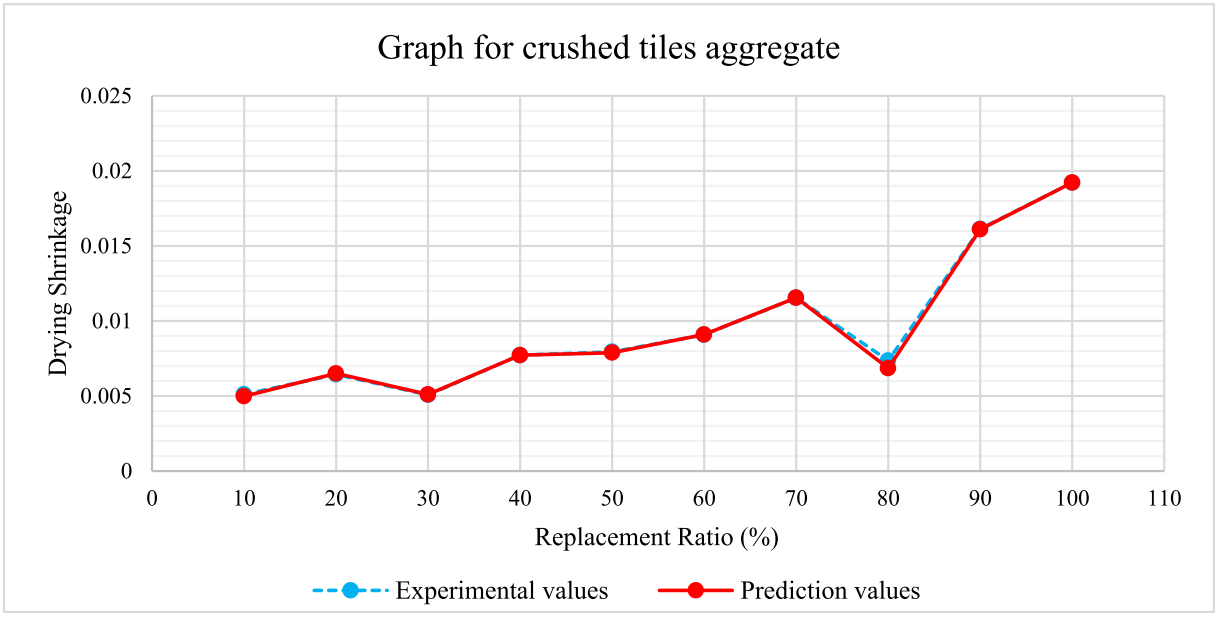

Fig. 15. Model prediction value and experimental value graph for drying shrinkage of CT aggregate based on replacement ratio.

related to both drying shrinkage values and drying shrinkage crack widths. The restraint level of drying shrinkage also affects the level or width values of drying shrinkage cracks. In this way, it seems that such properties of fine aggregates along with the replacement ratios also affect the performances of the developed models in accordance with both the natures of the actual problem and the machine learning algorithm. In summary, such approaches (not using only replacement ratios, using the properties of fine aggregates at the same time) may help to understand the experimental drying shrinkage cracking behaviors of mortars and the effects of fine aggregates on cracking in a different way. Graphs based on drying times tend to support this situation. The model was able to successfully predict both features with very high performance. It is seen that the model is successful in predicting different aggregate properties, but some aggregates are more prominent. In Fig. 23, comparative drying shrinkage graphs of all aggregates based on drying times are given, and in Fig. 24, crack width estimation graphs are given.

When the drying shrinkage and crack width prediction graphs of the aggregates in Figs. 23 and 24 were examined according to their

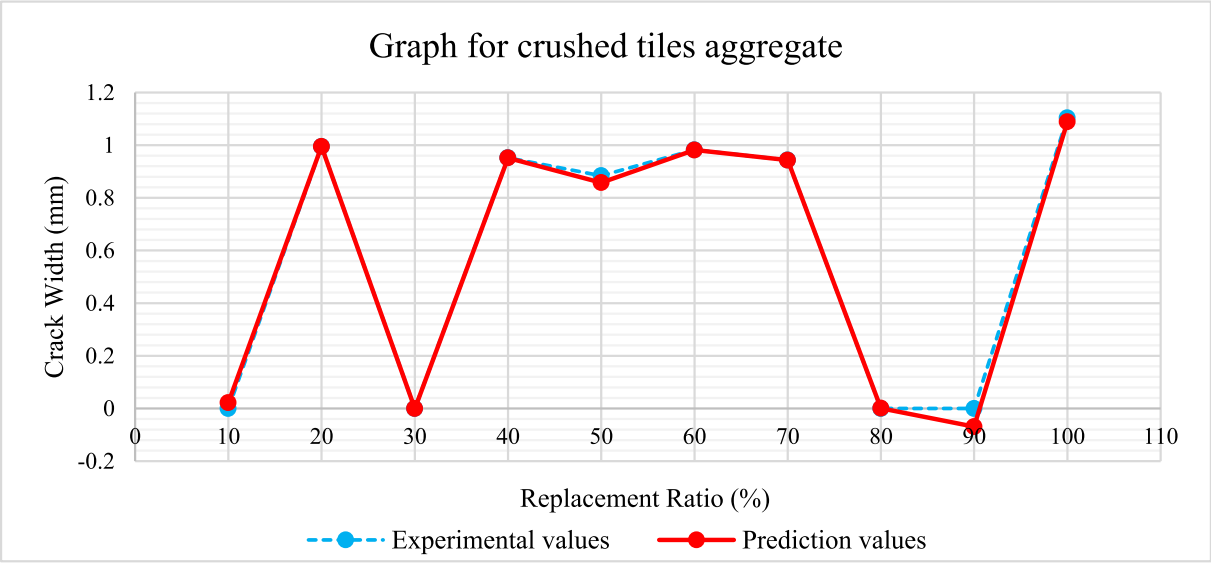

Fig. 16. Model prediction value and experimental value graph for crack width of CT aggregate based on replacement ratio.

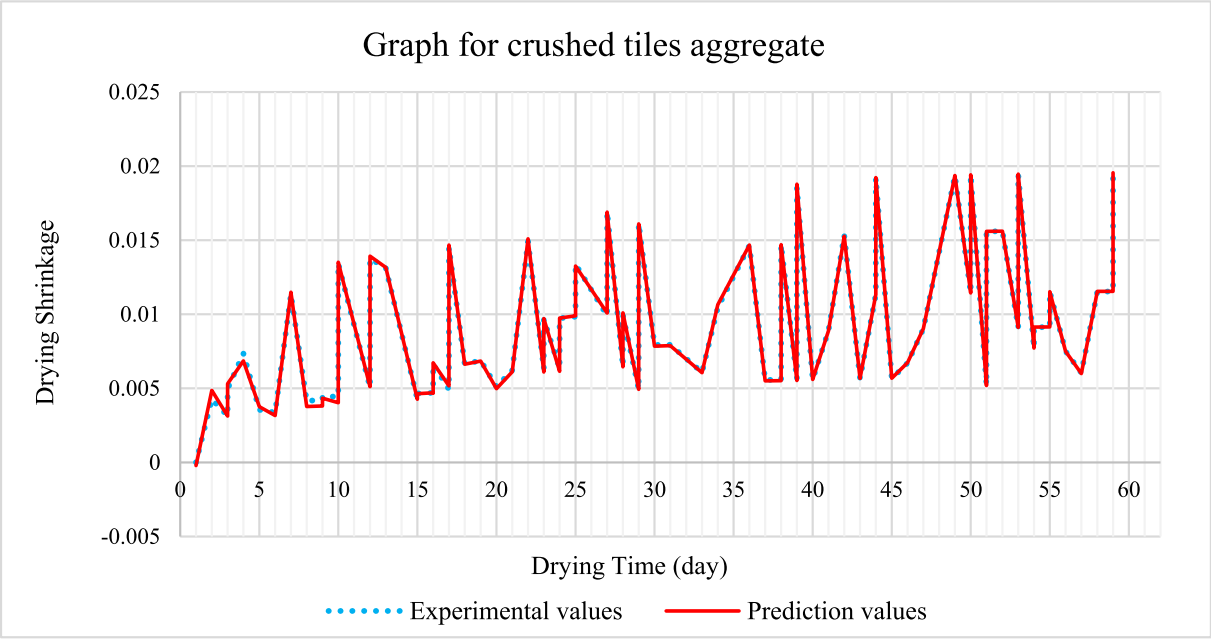

Fig. 17. Model prediction value and experimental value graph for drying shrinkage of CT aggregate based on drying time.

drying times, it was seen that the model produces prediction values that are generally compatible with the experimental values in all aggregates. According to the drying shrinkage graph in Fig. 23, while the performance of the model in predicting drying shrinkage shows a very close approach to the experimental values for BA, CT, and FA aggregate, it is seen that the predicted values for GBFS aggregate diverge from the experimental values by small amounts at some points. Accordingly, it can be said that the model performs more effectively in predicting drying shrinkage for the other 3 aggregates. According to the crack width model prediction graphs in Fig. 24, all aggregates generally produced predictions compatible with the experimental values. When examined on an aggregate basis, the model was more effective in predicting BA aggregate crack width and produced a prediction line similar to the experimental values. The other three aggregates gave similar results to each other. In the model, data on a certain number of aggregate types were used, but efficient results were obtained. Although there is no direct information on aggregate shape among the input parameters of the prediction model, results that cause differences in the performance evaluation of the model and indicate the effect of aggregate shape have been observed. The selected algorithm highlighted the features that distinguish the aggregates by categorizing the data while learning.

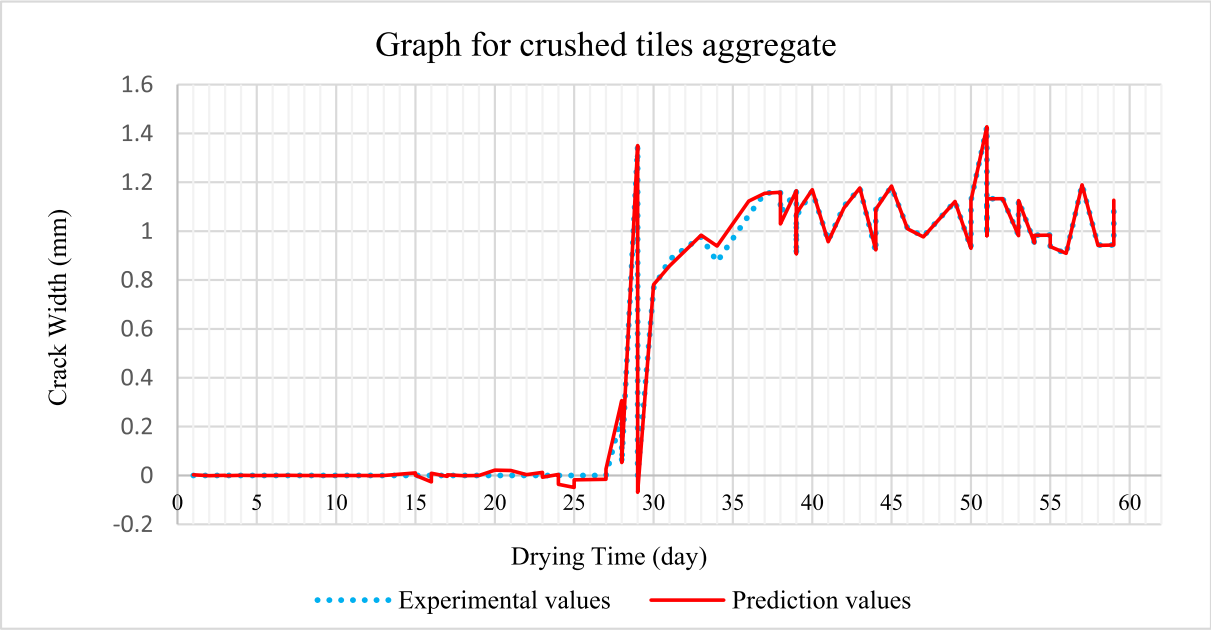

Fig. 18. Model prediction value and experimental value graph for crack width of CT aggregate based on drying time.

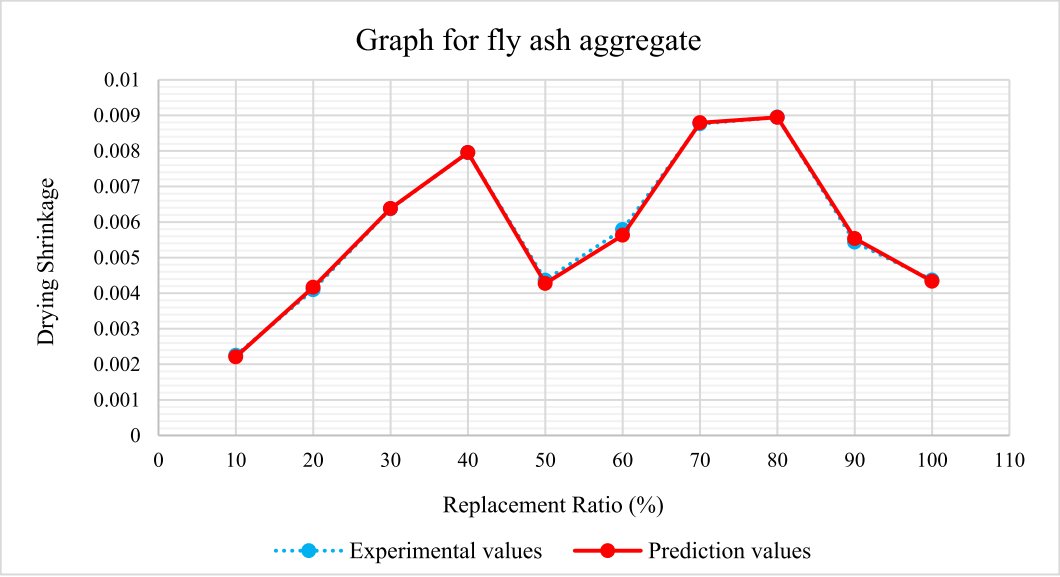

Fig. 19. Model prediction value and experimental value graph for drying shrinkage of FA aggregate based on replacement ratio.

However, this categorization may become difficult as the number of aggregates increases and contains aggregates with similar properties. Considering all these situations, in future studies, if the aggregate type is increased, it is recommended to try more than one machine learning algorithm and to use various information about aggregate properties as input to evaluate the performance of the model.

6. Conclusion

Developing technology has enabled the development of many artificial intelligence methods that save time and cost. Machine learning is an artificial intelligence tool that offers highly effective, economical, and fast solutions. Machine learning is frequently used in the field of civil engineering to ensure optimum efficiency in various experimental studies that require professional teams and equipment. This study aimed to predict the drying shrinkage and widths of cracks that will occur in the concrete after the use of various

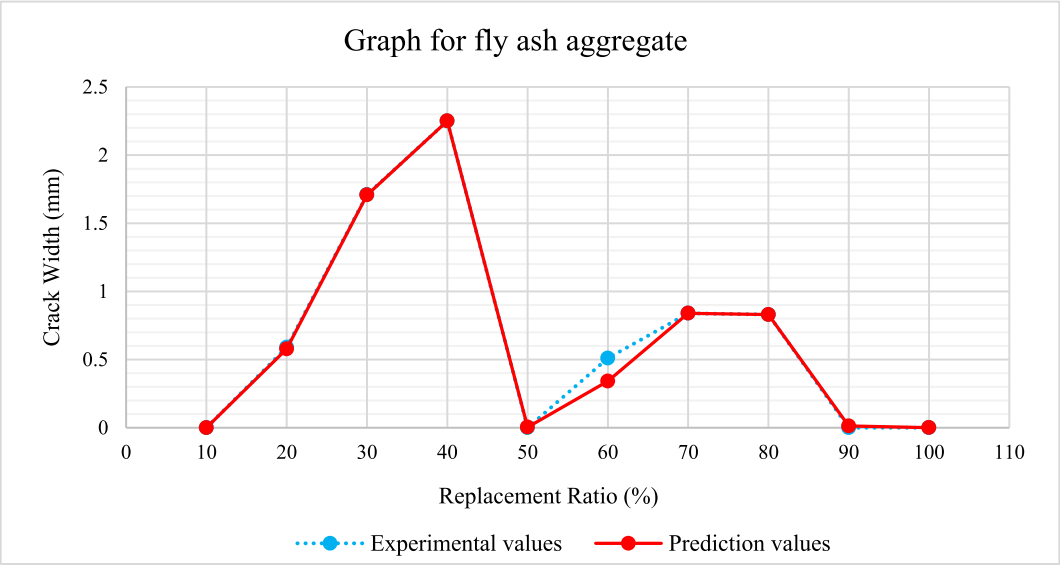

Fig. 20. Model prediction value and experimental value graph for crack width of FA aggregate based on replacement ratio.

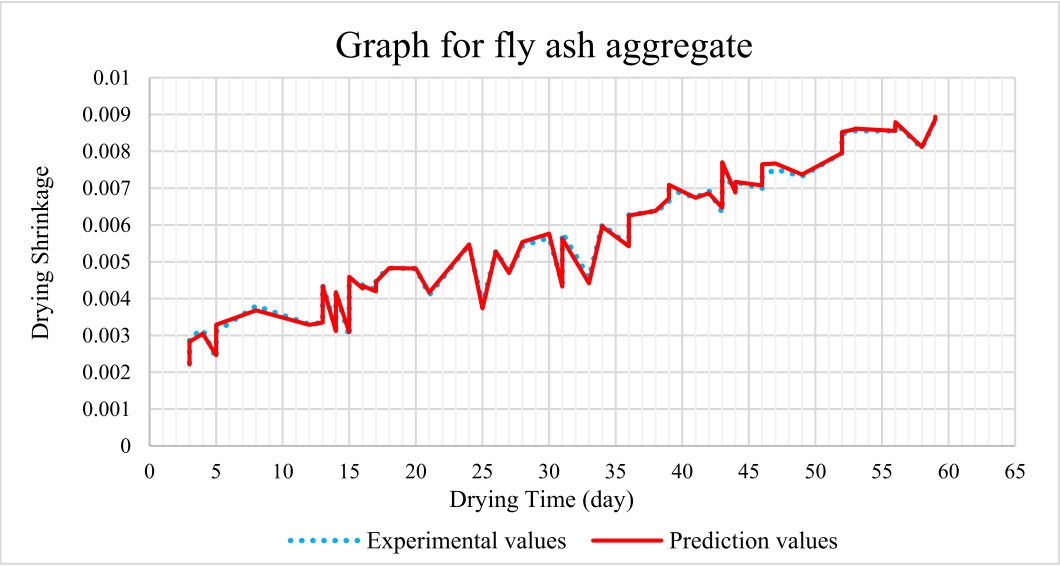

Fig. 21. Model prediction value and experimental value graph for drying shrinkage of FA aggregate based on drying time.

aggregates such as waste or sub-industrial products, with the help of machine learning. In this study, the results obtained from 60-day experimental measurements of concrete mortars with different aggregate substitution rates formed the data set and later a prediction model for estimation of drying shrinkage and widths of cracks was developed. 12 machine learning algorithms were evaluated during the development process. Among the algorithms tested, Decision Tree, XGBoost, Random Forest, Bagging and CatBoost algorithms were able to provide a prediction performance exceeding 99 %. Among them, CatBoost emerged as the best algorithm with an average R2 score of 99.59 %. Later the performance of the model was improved by optimizing the CatBoost algorithm's hyperparameters. The CatBoost model with optimal hyperparameters was a superior predictor with a mean R2 score of 99.66 %. CatBoost(CB) is an algorithm developed by search engine company Yandex in 2017. CatBoost is based on decision trees and gradient boosting and grows a special type of trees (symmetric/oblivious trees) which allows for a simple fitting scheme and efficiency on CPUs with a tree structure itself working as a regularization. CatBoost provides an unusual method of dealing with categorical data, requiring not much categorical feature transformation [95]. Although the data used in our cases is totally numeric, the success of the CatBoost Regressor can be strongly related to the algorithm's efficiency in utilizing the CPU and its flexibility which allows efficient adjustment of its hyper-parameters. CatBoost offers a natural way of regularization, but the regularization ability of CatBoost might not be positively affecting the success of CatBoost for this dataset, as the accuracy achieved by key regularization enablers Lasso, Ridge, and ElasticNet appeared

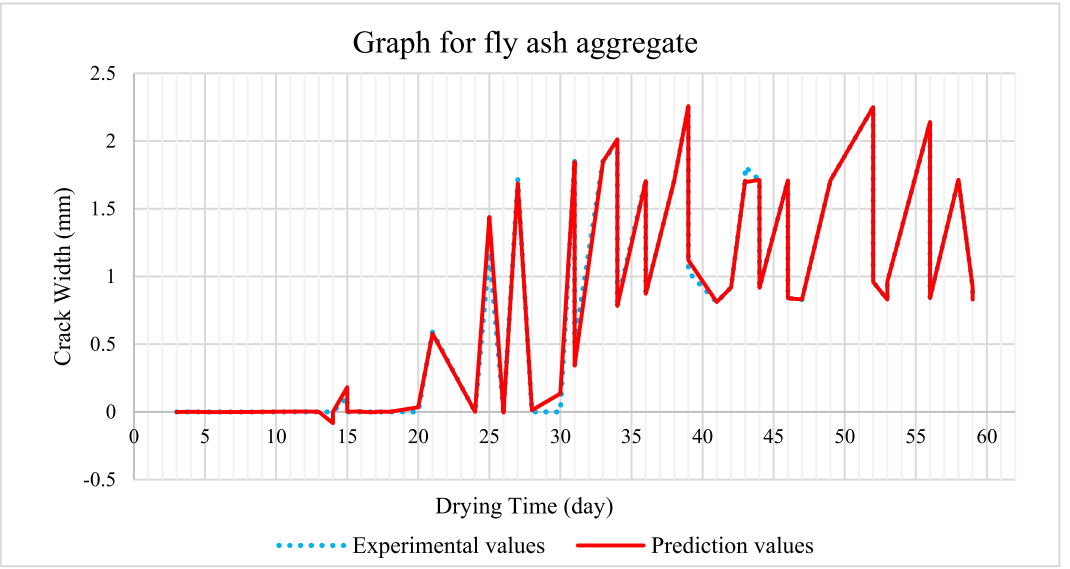

Fig. 22. Model prediction value and experimental value graph for crack width of FA aggregate based on drying time.

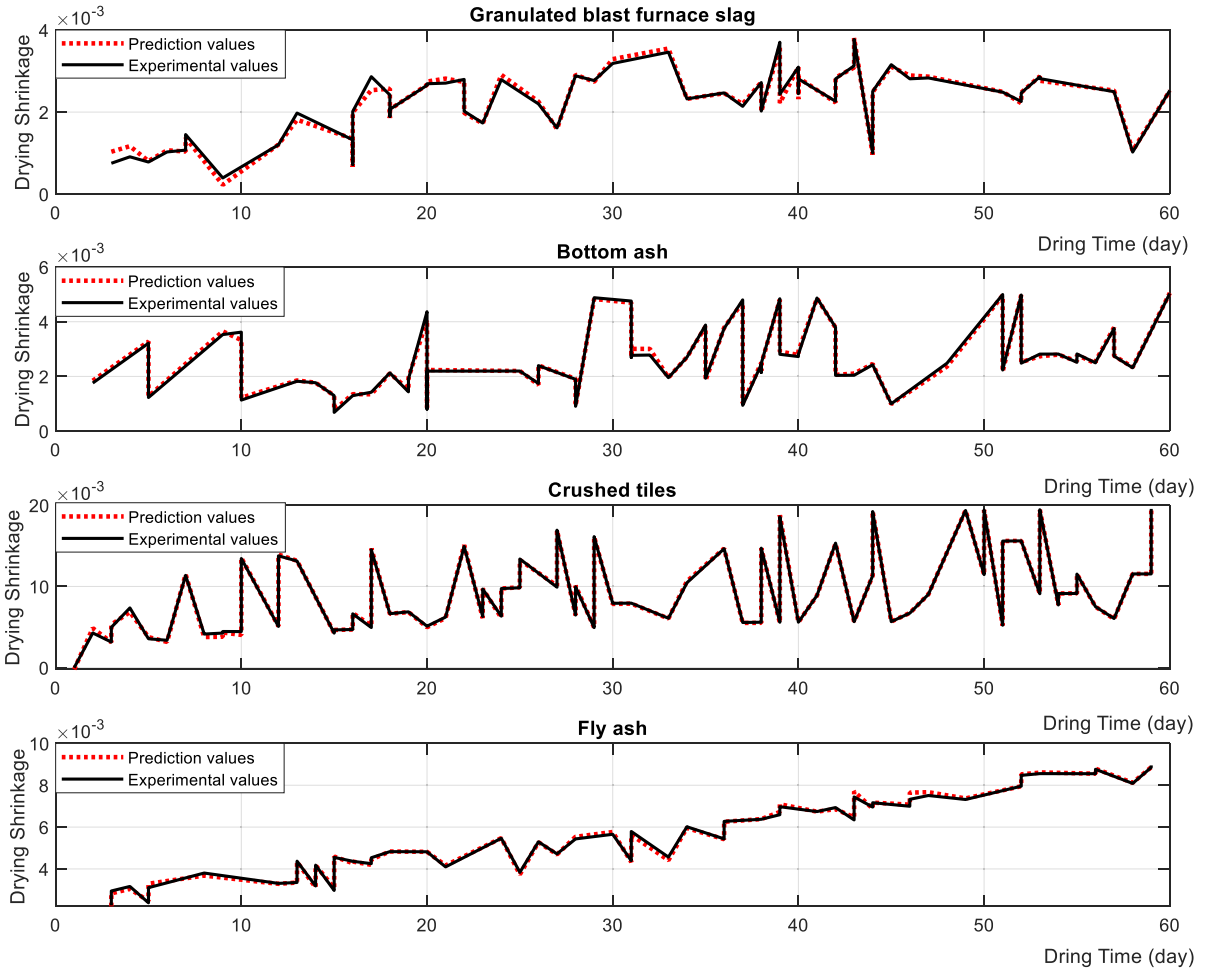

Fig. 23. Model predicted value and experimental value graphs for drying shrinkage based on the drying time of all aggregates.

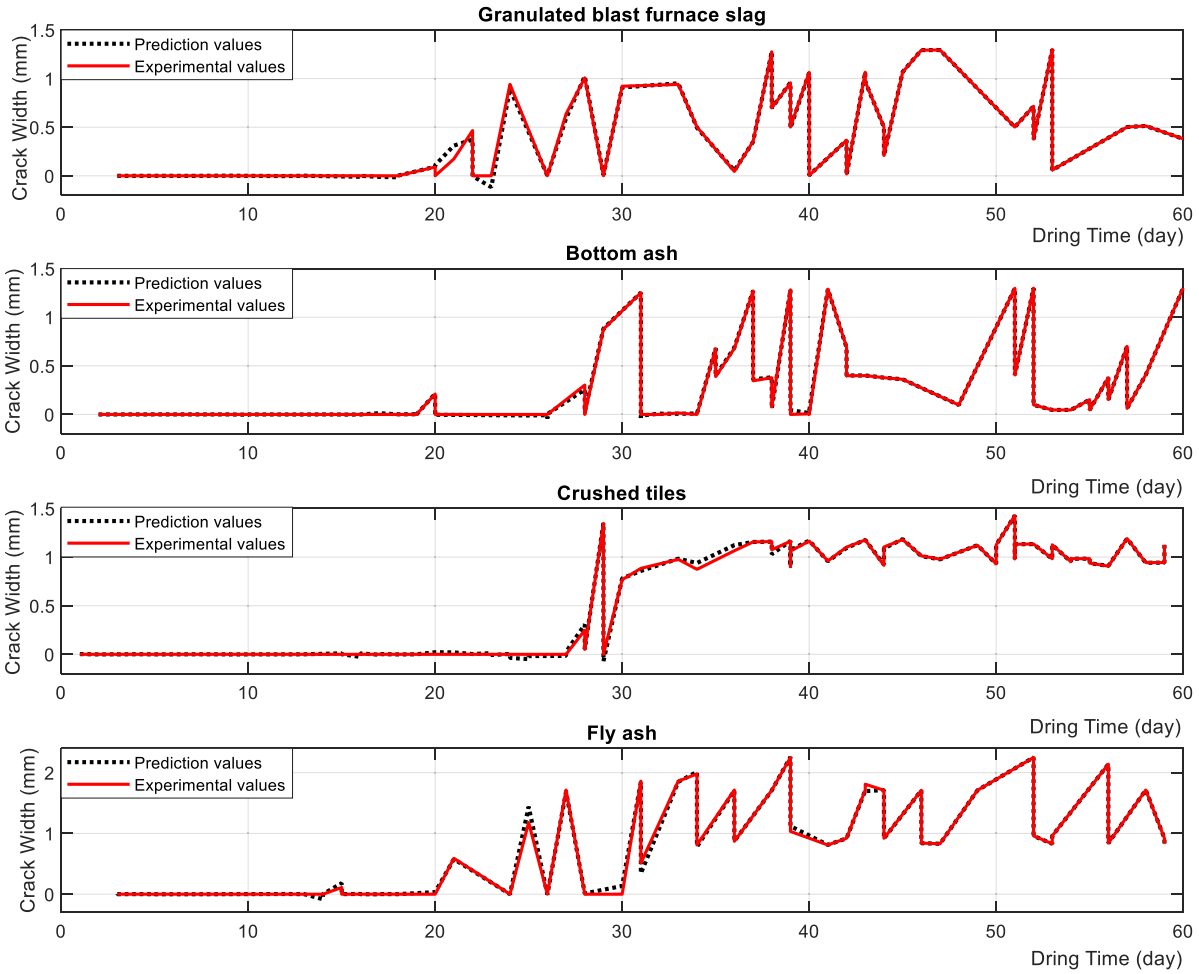

Fig. 24. Model predicted value and experimental value graphs for crack width based on the drying time of all aggregates.

as the lowest ones for the dataset. Another reason behind the effective success of the CatBoost algorithm in this problem may be that the values of the aggregates, such as tensile and compressive strength, repeat in a certain order in the data. Although the aggregates used in the study do not specify a category, they pointed to a certain aggregate with their unique measured compressive and tensile strength properties. While the machine was learning the data, it may have captured this order within itself and perceived it as numerical data that behaves as if it were categorical according to these features. This situation may enable the CatBoost algorithm to obtain better results for the numerical fields. Furthermore, even if the properties of aggregate numerically measured via experimental procedures (or the linguistic definitions for these aggregates have not been included in CBR or NCBR ML models), an interesting fact has been observed as fine aggregate physical shape (angular or round) seems to be effective on predicting drying shrinkage deformations or crack widths. Besides, along with the replacement ratios and mixture proportions (ingredient or component contents), the linguistic or numerical properties of each component also may affect the prediction performances of different ML algorithm models. In this case, the NCBR model has been specific for the drying shrinkage properties of these fine aggregate mortars. On the other hand, it is possible to generalize this model for drying shrinkage and drying shrinkage cracking properties, or for other fresh and hardened properties of different mortar or concrete types, which incorporate different cement and aggregate types, via some additional experimental studies.

The results of the research demonstrated that studies on estimating the drying shrinkage and crack width, which require long experimental observations, can be facilitated by machine learning models trained with data acquired from past studies and experiments, and shrinkage and crack width can be determined with high accuracy with machine learning models. As a result of the study, it is recommended to consider some characteristics of the aggregates such as chemical, physical or mechanical properties (particle size distribution-granulometry, chemical compositions, fineness, water absorption, surface texture and shape, maximum aggregate size, water absorption, permeability, porosity, density, unit weight, abrasion resistance, etc.), increase the number of types of aggregates included for modelling drying shrinkage and crack widhts, and re-evaluate the algorithm performances to be used in the development of the prediction model. The results contain clues that the physical properties of the aggregates used in the model are effective in the

prediction performance. In the current study, a prediction model was developed with a limited number of aggregate types, without including aggregate physical properties. For a more general model, the importance of including physical properties such as aggregate shape is understood. The CatBoost algorithm managed to successfully categorize the aggregates used in the study. However, the increase in aggregate types and properties may make this categorization difficult and may be insufficient, especially in estimating aggregates with similar properties. Considering this situation, it is anticipated that the most effective algorithm should be re-examined after more parameters are included in the model.

CRediT authorship contribution statement

Ayla Ocak: Writing – original draft, Methodology, Formal analysis. **Gebrail Bekdaş:** Writing – review & editing, Supervision, Methodology, Conceptualization. **Ümit Işıkdağ:** Writing – original draft, Validation, Supervision, Methodology, Formal analysis. **Sinan Melih Nigdeli:** Writing – review & editing, Supervision. **Turhan Bilir:** Writing – review & editing, Writing – original draft, Data curation.

Declaration of competing interest

The authors declare that they have no known competing financial interests or personal relationships that could have appeared to influence the work reported in this paper.

Data availability

Data will be made available on request.

References

[1] T. Bilir, The Effects of Industrial By-Products or Wastes as Fine Aggregate on Drying Shrinkage Cracking of Mortars, MSc, Eskisehir Osmangazi University. Institute of Science and Technology, Eskisehir, 2010. Thesis.
[2] A.M. Ghaly, M.S. Gill, Compression and deformation performance of concrete containing post-consumer plastics, J. Mater. Civ. Eng. 16 (4) (2004) 289–296.
[3] F.M. Khalaf, A.S. DeVenny, Properties of new and recycled clay brick aggregates for use in concrete, J. Mater. Civ. Eng. 17 (4) (2005) 456–464.
[4] D.C.L. Teo, M.A. Mannan, V.J. Kurian, Structural concrete using oil palm shell (OPS) as lightweight aggregate, Turk. J. Eng. Environ. Sci. 30 (4) (2006).
[5] D. Roy, Suitability of blast furnace slag as coarse aggregate in concrete, Journal of the Institution of Engineers. India. Civil Engineering Division 88 (5) (2007) 57–61.
[6] A.R. Khaloo, M. Dehestani, P. Rahmatabadi, Mechanical properties of concrete containing a high volume of tire–rubber particles, Waste Manag. 28 (12) (2008) 2472–2482.
[7] M.L. Berndt, Properties of sustainable concrete containing fly ash, slag, and recycled concrete aggregate, Construct. Build. Mater. 23 (7) (2009) 2606–2613.
[8] S. Akçaözoğlu, C.D. Atiş, K. Akçaözoğlu, An investigation on the use of shredded waste PET bottles as aggregate in lightweight concrete, Waste Manag. 30 (2) (2010) 285–290.
[9] H. Hebhoub, H. Aoun, M. Belachia, H. Houari, E. Ghorbel, Use of waste marble aggregates in concrete, Construct. Build. Mater. 25 (3) (2011) 1167–1171.
[10] K.B. Najim, M.R. Hall, Mechanical and dynamic properties of self-compacting crumb rubber modified concrete, Construct. Build. Mater. 27 (1) (2012) 521–530.
[11] M. Vijayalakshmi, A.S.S. Sekar, Strength and durability properties of concrete made with granite industry waste, Construct. Build. Mater. 46 (2013) 1–7.
[12] H. Dilbas, M. Şimşek, Ö. Çakır, An investigation on mechanical and physical properties of recycled aggregate concrete (RAC) with and without silica fume, Construct. Build. Mater. 61 (2014) 50–59.
[13] C.J. Lynn, R.K. Dhir, G.S. Ghataora, R.P. West, Sewage sludge ash characteristics and potential for use in concrete, Construct. Build. Mater. 98 (2015) 767–779.
[14] A.U. Shettima, M.W. Hussin, Y. Ahmad, J. Mirza, Evaluation of iron ore tailings as replacement for fine aggregate in concrete, Construct. Build. Mater. 120 (2016) 72–79.
[15] L. Mo, F. Zhang, M. Deng, F. Jin, A. Al-Tabbaa, A. Wang, Accelerated carbonation and performance of concrete made with steel slag as binding materials and aggregates, Cement Concr. Compos. 83 (2017) 138–145.
[16] R.K. Majhi, A.N. Nayak, B.B. Mukharjee, Development of sustainable concrete using recycled coarse aggregate and ground granulated blast furnace slag, Construct. Build. Mater. 159 (2018) 417–430.
[17] J.X. Lu, X. Yan, P. He, C.S. Poon, Sustainable design of pervious concrete using waste glass and recycled concrete aggregate, J. Clean. Prod. 234 (2019) 1102–1112.
[18] S.C. Bostanci, Use of waste marble dust and recycled glass for sustainable concrete production, J. Clean. Prod. 251 (2020) 119785.
[19] S. Gao, G. Zhao, L. Guo, L. Zhou, K. Yuan, Utilization of coal gangue as coarse aggregates in structural concrete, Construct. Build. Mater. 268 (2021) 121212.
[20] A.İ. Çelik, Y.O. Özkılıç, Ö. Zeybek, M. Karalar, S. Qaidi, J. Ahmad, C. Bejinariu, Mechanical behavior of crushed waste glass as replacement of aggregates, Materials 15 (22) (2022) 8093.
[21] Z. Li, W. Zhang, H. Jin, X. Fan, J. Liu, F. Xing, L. Tang, Research on the durability and Sustainability of an artificial lightweight aggregate concrete made from municipal solid waste incinerator bottom ash (MSWIBA), Construct. Build. Mater. 365 (2023) 129993.
[22] N.M.S. Hasan, M.H.R. Sobuz, N.M.N. Shaurdho, M.A. Basit, S.C. Paul, M.M. Meraz, M.J. Miah, Investigation of lightweight and green concrete characteristics using coconut shell aggregate as a replacement for conventional aggregates, Int. J. Civ. Eng. (2023) 1–17.
[23] I.B. Topçu, T. Bilir, Effect of bottom ash as fine aggregate on shrinkage cracking of mortars, ACI Mater. J. 107 (1) (2010) 48.
[24] I.B. Topçu, T. Bilir, Effect of non-ground-granulated blast-furnace slag as fine aggregate on shrinkage cracking of mortars, ACI Mater. J. 107 (6) (2010).
[25] İ.B. Topçu, T. Bilir, Experimental investigation of drying shrinkage cracking of composite mortars incorporating crushed tile fine aggregate, Mater. Des. 31 (9) (2010) 4088–4097.
[26] T. Bilir, O. Gencel, I.B. Topcu, Properties of mortars with fly ash as fine aggregate, Construct. Build. Mater. 93 (2015) 782–789.
[27] T. Bilir, O. Gencel, I.B. Topcu, Prediction of restrained shrinkage crack widths of slag mortar composites by Takagi and Sugeno ANFIS models, Neural Comput. Appl. 27 (2016) 2523–2536.
[28] W.J. Weiss, S.P. Shah, Recent trends to reduce shrinkage cracking in concrete pavements, in: Proceedings of the 1997 Airfield Pavement Conference, 1997, December.
[29] K. Raoufi, J. Weiss, The role of fiber reinforcement in mitigating shrinkage cracks in concrete, in: Fibrous and Composite Materials for Civil Engineering Applications, Woodhead Publishing, 2011, pp. 168–188.
[30] K.J. Folliard, N.S. Berke, Properties of high-performance concrete containing shrinkage-reducing admixture, Cement Concr. Res. 27 (9) (1997) 1357–1364.
[31] S. Nagataki, H. Gomi, Expansive admixtures (mainly ettringite), Cement Concr. Compos. 20 (2–3) (1998) 163–170.
[32] M. Cyr, C. Ouyang, S.P. Shah, Design of hybrid-fiber reinforcement for shrinkage cracking by crack width predictions, Brittle Matrix Compos 7 (2003) 243–252.

[33] M. Collepardi, A. Borsoi, S. Collepardi, J.J.O. Olagot, R. Troli, Effects of shrinkage reducing admixture in shrinkage compensating concrete under non-wet curing conditions, Cement Concr. Compos. 27 (6) (2005) 704–708.
[34] H.R. Shah, J. Weiss, Quantifying shrinkage cracking in fiber-reinforced concrete using the ring test, Mater. Struct. 39 (2006) 887–899.
[35] Z. Konik, J. Małolepszy, W. Roszczynialski, A. Stok, Production of expansive additive to Portland cement, J. Eur. Ceram. Soc. 27 (2–3) (2007) 605–609.
[36] G. Barluenga, F. Hernández-Olivares, Cracking control of concretes modified with short AR-glass fibers at an early age. Experimental results on standard concrete and SCC, Cement Concr. Res. 37 (12) (2007) 1624–1638.
[37] L. Mo, M. Deng, M. Tang, A. Al-Tabbaa, MgO expansive cement and concrete in China: past, present and future, Cement Concr. Res. 57 (2014) 1–12.
[38] D. Shen, C. Wen, J. Kang, H. Shi, Z. Xu, Early-age stress relaxation and cracking potential of High-strength concrete reinforced with Barchip fiber, Construct. Build. Mater. 258 (2020) 119538.
[39] M. Gholami, F. Moghadas Nejad, A.M. Ramezanianpour, Increasing the length of concrete pavement slabs using shrinkage-reducing reducing admixture and polypropylene fiber, International Journal of Concrete Structures and Materials 18 (1) (2024) 9.
[40] A. Zielinski, M. Kaszynska, Assessment of cracking potential of normal - and lightweight self-consolidating concrete, in: In Proceedings of the 10th Fib International PhD Symposium in Civil Engineering, 2014, pp. 103–108.
[41] E. Güneyisi, M. Gesoglu, O.A. Azez, H.Ö. Öz, Physico-mechanical properties of self-compacting concrete containing treated cold-bonded fly ash lightweight aggregates and SiO2 nano-particles, Construct. Build. Mater. 101 (2015) 1142–1153.
[42] E. Lee, S. Park, Y. Kim, Drying shrinkage cracking of concrete using dune sand and crushed sand, Construct. Build. Mater. 126 (2016) 517–526.
[43] Y. Yu, H. Zhu, Influences of rubber on drying shrinkage performance of cement-based materials, Fuhe Cailiao Xuebao/Acta Materiae Compositae Sinica 34 (11) (2017) 2624–2630.
[44] J. Gong, W. Zeng, W. Zhang, Influence of shrinkage-reducing agent and polypropylene fiber on shrinkage of ceramsite concrete, Construct. Build. Mater. 159 (2018) 155–163.
[45] M. Maghfouri, P. Shafigh, V. Alimohammadi, Drying shrinkage strain development of agro-waste oil palm shell lightweight aggregate concrete by using the experimental result, ACI, and Eurocode prediction models, International Journal of Integrated Engineering 11 (9 Special Issue) (2019) 255–263.
[46] D. Zhang, P. Han, Q. Yang, M. Mao, Shrinkage effects of using fly ash instead of fine aggregate in concrete mixtures, Adv. Mater. Sci. Eng. 2020 (2020) 1–11.
[47] L.V. Hung, L.T. Thanh, N. Van Tuan, Experimental study on drying shrinkage of structural lightweight concrete using fly ash cenospheres, Int. J. GEOMATE 21 (87) (2021) 95–101.
[48] T.P. Huynh, L.S. Ho, Q. Van Ho, Experimental investigation on the performance of concrete incorporating fine dune sand and ground granulated blast-furnace slag, Construct. Build. Mater. 347 (2022) 128512.
[49] Z. Nasser Eddine, F. Barraj, J. Khatib, A. Elkordi, Volume stability of pervious concrete pavement containing municipal solid waste incineration bottom ash, International Journal of Pavement Research and Technology (2023) 1–14.
[50] J. Shi, W. Pan, J. Kang, Z. Yu, G. Sun, J. Li, J. Shen, Properties of Ultra-High Performance Concrete incorporating iron tailings powder and iron tailings sand, J. Build. Eng. 83 (2024) 108442.
[51] M. Liang, Z. Chang, Z. Wan, Y. Gan, E. Schlangen, B. Šavija, Interpretable Ensemble-Machine-Learning models for predicting creep behavior of concrete, Cement Concr. Compos. 125 (2022) 104295.
[52] Y. Ren, J. Huang, Z. Hong, W. Lu, J. Yin, L. Zou, X. Shen, Image-based concrete crack detection in tunnels using deep fully convolutional networks, Construct. Build. Mater. 234 (2020) 117367.
[53] D.C. Feng, Z.T. Liu, X.D. Wang, Y. Chen, J.Q. Chang, D.F. Wei, Z.M. Jiang, Machine learning-based compressive strength prediction for concrete: an adaptive boosting approach, Construct. Build. Mater. 230 (2020) 117000.
[54] D.K. Bui, T. Nguyen, J.S. Chou, H. Nguyen-Xuan, T.D. Ngo, A modified firefly algorithm-artificial neural network expert system for predicting compressive and tensile strength of high-performance concrete, Construct. Build. Mater. 180 (2018) 320–333.
[55] P.G. Asteris, A.D. Skentou, A. Bardhan, P. Samui, K. Pilakoutas, Predicting concrete compressive strength using hybrid ensembling of surrogate machine learning models, Cement Concr. Res. 145 (2021) 106449.
[56] A. Behnood, E.M. Golafshani, Machine learning study of the mechanical properties of concretes containing waste foundry sand, Construct. Build. Mater. 243 (2020) 118152.
[57] W.B. Chaabene, M. Flah, M.L. Nehdi, Machine learning prediction of mechanical properties of concrete: critical review, Construct. Build. Mater. 260 (2020) 119889.
[58] I. Nunez, M.L. Nehdi, Machine learning prediction of carbonation depth in recycled aggregate concrete incorporating SCMs, Construct. Build. Mater. 287 (2021) 123027.
[59] K. Liu, M.S. Alam, J. Zhu, J. Zheng, L. Chi, Prediction of carbonation depth for recycled aggregate concrete using ANN hybridized with swarm intelligence algorithms, Construct. Build. Mater. 301 (2021) 124382.
[60] Y. Lou, H. Wang, M.N. Amin, S.U. Arifeen, Y. Dodo, F. Althoey, A.F. Deifalla, Predicting the crack repair rate of self-healing concrete using soft-computing tools, Mater. Today Commun. 38 (2024) 108043.
[61] X. Yuan, Q. Cao, M.N. Amin, A. Ahmad, W. Ahmad, F. Althoey, A.F. Deifalla, Predicting the crack width of the engineered cementitious materials via standard machine learning algorithms, J. Mater. Res. Technol. 24 (2023) 6187–6200.
[62] S. Dorafshan, R.J. Thomas, M. Maguire, Comparison of deep convolutional neural networks and edge detectors for image-based crack detection in concrete, Construct. Build. Mater. 186 (2018) 1031–1045.
[63] G. Bayar, T. Bilir, A novel study for the estimation of crack propagation in concrete using machine learning algorithms, Construct. Build. Mater. 215 (2019) 670–685.
[64] S.O. Abioye, L.O. Oyedele, L. Akanbi, A. Ajayi, J.M.D. Delgado, et al., Artificial intelligence in the construction industry: a review of present status, opportunities, and future challenges, J. Build. Eng. 44 (2021) 103299.
[65] S.B. Kotsiantis, I. Zaharakis, P. Pintelas, Supervised machine learning: a review of classification techniques, Emerging Artificial Intelligence Applications in Computer Engineering 160 (1) (2007) 3–24.
[66] N. Zincir-Heywood, M. Mellia, Y. Diao, Overview of artificial intelligence and machine learning, Communication Networks and Service Management in the Era of Artificial Intelligence and Machine Learning (2021) 19–32.
[67] R.S. Sutton, Introduction: the challenge of reinforcement learning, in: Reinforcement Learning, Springer, Boston, MA, 1992, pp. 1–3.
[68] A.G. Barto, T.G. Dietterich, Reinforcement learning and its relationship to supervised learning, in: Handbook of Learning and Approximate Dynamic Programming, vol. 10, 9780470544785, 2004.
[69] A. Ocak, S.M. Nigdeli, G. Bekdaş, Ü. Işıkdağ, Artificial intelligence and deep learning in civil engineering, in: Hybrid Metaheuristics in Structural Engineering: Including Machine Learning Applications, Springer Nature Switzerland, Cham, 2023, pp. 265–288.
[70] P. Nitsche, R. Stütz, M. Kammer, P. Maurer, Comparison of machine learning methods for evaluating pavement roughness based on vehicle response, J. Comput. Civ. Eng. 28 (4) (2014) 04014015.
[71] Y. Zhao, Y. Zhang, Comparison of decision tree methods for finding active objects, Adv. Space Res. 41 (12) (2008) 1955–1959.
[72] R. Nyirandayisabye, H. Li, Q. Dong, T. Hakuzweyezu, F. Nkinahamira, Automatic pavement damage predictions using various machine learning algorithms: evaluation and comparison, Results in Engineering 16 (2022) 100657.
[73] A. Hashemizadeh, A. Maaref, M. Shateri, A. Larestani, A. Hemmati-Sarapardeh, Experimental measurement and modeling of water-based drilling mud density using adaptive boosting decision tree, support vector machine, and K-nearest neighbors: a case study from the South Pars gas field, J. Petrol. Sci. Eng. 207 (2021) 109132.
[74] O. Anava, K. Levy, K*-nearest neighbors: from global to local, Adv. Neural Inf. Process. Syst. 29 (2016).
[75] A. Sivasubramanian, S.A. Krishna, D.H. Nair, K. Varma, R. Radhakrishnan, D. Sathyan, Experimental validation of compressive strength prediction using machine learning algorithm, Mater. Today: Proc. 64 (2022) 181–187.

[76] A.P. Rodrigues, R. Fernandes, P. Vijaya, A study on the evaluation of different regressors in Weather Prediction, in: 2022 International Conference on Artificial Intelligence and Data Engineering (AIDE), IEEE, 2022, December, pp. 13–18.
[77] A. Afzal, S. Alshahrani, A. Alrobaian, A. Buradi, S.A. Khan, Power plant energy predictions based on thermal factors using ridge and support vector regressor algorithms, Energies 14 (21) (2021) 7254.
[78] S. Kumar, M.K. Goyal, V. Deshpande, M. Agarwal, Estimation of time-dependent scour depth around circular bridge piers: application of ensemble machine learning methods, Ocean Eng. 270 (2023) 113611.
[79] M.S.I. Khan, N. Islam, J. Uddin, S. Islam, M.K. Nasir, Water quality prediction and classification based on principal component regression and gradient boosting classifier approach, Journal of King Saud University-Computer and Information Sciences 34 (8) (2022) 4773–4781.
[80] M. Khan, W. Anwar, M. Rasheed, T. Najeh, Y. Gamil, F. Farooq, Forecasting the strength of graphene nanoparticles-reinforced cementitious composites using ensemble learning algorithms, Results in Engineering (2024) 101837.
[81] F.A. Musleh, A comparative study to forecast the total nitrogen effluent concentration in a wastewater treatment plant using machine learning techniques, International Journal of Computing and Digital Systems 14 (1) (2023) 10447–10456.
[82] XGBoost Developers, XGBoost Python package. https://pypi.org/project/XGBoost/1.7.2/, 2022.
[83] R.K. Tipu, V.R. Panchal, K.S. Pandya, Multi-objective optimized high-strength concrete mix design using a hybrid machine learning and metaheuristic algorithm, Asian Journal of Civil Engineering 24 (3) (2023) 849–867.
[84] G. Ke, Q. Meng, T. Finley, T. Wang, W. Chen, W. Ma, T.Y. Liu, Lightgbm: a highly efficient gradient-boosting decision tree, Adv. Neural Inf. Process. Syst. 30 (2017).
[85] A. Shehadeh, O. Alshboul, R.E. Al Mamlook, O. Hamedat, Machine learning models for predicting the residual value of heavy construction equipment: an evaluation of modified decision tree, LightGBM, and XGBoost regression, Autom. ConStruct. 129 (2021) 103827.
[86] S.K. Panda, S.N. Mohanty, Time series forecasting and modeling of food demand supply chain based on regressors analysis, IEEE Access (2023).
[87] CatBoost Developers, Catboost Python package. https://pypi.org/project/catboost/, 2022.
[88] A.V. Dorogush, V. Ershov, A. Gulin, in: CatBoost: Gradient Boosting with Categorical Features Support, 2018 *arXiv preprint arXiv:1810.11363*.
[89] J. Ko, Y.C. Byun, Analyzing factors affecting micro-mobility and predicting micro-mobility demand using ensemble voting regressor, Electronics 12 (21) (2023) 4410.
[90] Optuna Developers, Optuna: a hyperparameter optimization framework Python package. https://pypi.org/project/optuna/, 2023.
[91] S. Geisser, W.F. Eddy, A predictive approach to model selection, J. Am. Stat. Assoc. 74 (365) (1979) 153–160.
[92] W. Zhang, C. Wu, Y. Li, L. Wang, P. Samui, Assessment of pile drivability using random forest regression and multivariate adaptive regression splines, Georisk 15 (1) (2021) 27–40.
[93] F. Pedregosa, G. Varoquaux, A. Gramfort, V. Michel, B. Thirion, et al., Scikit-learn: machine learning in Python. https://scikit-learn.org/stable/about.html#citing-scikit-learn, 2022.
[94] https://catboost.ai/en/docs/concepts/parameter-tuning, [Date of Visit: April 7, 2024].
[95] https://catboost.ai/news/catboost-enables-fast-gradient-boosting-on-decision-trees-using-gpus.